INFLUENCE OF PARITY ON UTERINE STRUCTURE IN PREGNANT RABBITS: A LIGHT MICROSCOPY AND IMMUNOHISTOCHEMICAL STUDY

Dr. Anne Naipanoi Pulei

A thesis submitted in partial fulfillment of the requirements for the degree of Master of Science in Human Anatomy, University of Nairobi.

DECLARATION

I hereby confirm that this thesis represents my original work and has not been presented for examination elsewhere.

Candidate:

Sign: ----------Date: ----------

Dr. Anne N. Pulei, BSc. (Anat), MBChB

Department of Human Anatomy, University of Nairobi

This thesis is presented with our approval as university supervisors:

Sign: ---------- Date: ----------

Prof. Peter Gichangi, BSc. (Anat), MBChB, MMed (Obs/Gyn), PhD

Department of Human Anatomy, University of Nairobi

Sign: ---------- Date: ----------

Dr. Andrew Makanya, BVM, MSc, DVM, PhD

Department of Veterinary Anatomy and Physiology, University of Nairobi

Sign: ----------Date: ----------

Prof. Julius Ogeng'o, BSc. (Anat), MBChB, PhD

Department of Human Anatomy, University of Nairobi

DEDICATIONS

This work is dedicated to my parents Mr. Francis Pulei and Mrs. Lois Pulei, my siblings; Alex Lengete Pulei, Nancy Nampa Pulei and Steven Sampao Pulei as well as my grandmother Mrs. Noonkota Munkush, for their endless support.

In memory of Mrs. Naimado Kapaito and Mr. Nooridon Munkush: you left fingerprints of grace in our lives. You shall not be forgotten.

ACKNOWLEDGEMENTS

I would like to express my uttermost gratitude to my supervisors Prof. Julius Ogeng'o, Dr Andrew Makanya and Dr. Peter Gichangi for their inspiration as well as their surpassing guidance during the entire research period. I also thank Prof. Saidi Hassan, Dr. Pamela Mandela and Dr. Kevin Ongeti for their helpful advice and ideas. I specifically acknowledge Dr. Pamela Mandela for editing this thesis. I wish to acknowledge the assistance provided by our laboratory technicians especially Ms. Sarah Mungania, Mr. Christopher Kamwaro, Mr. Peter Nzioka, Mrs. Judy Machira, Mrs. Esther Mburu and Ms. Margaret Irungu. I am incredibly grateful to Mr. Joseph Mwaniki and Mr. Joseph Moseti from the Departments of Biochemistry and Medical Physiology respectively, for their devoted support in caring for the experimental animals. I am greatly indebted to Poonamnjit Loyal for her devoted assistance during data analysis. I appreciate my classmate Dr. Beda Otieno for our time together, support and contagious working spirit. Lastly, I wish to express my gratitude to Dr. Josephine Mwikali Ndolo and Dr. Wanjiku Ndung'u for their enduring support.

TABLE OF CONTENTS

LIST OF FIGURES

LIST OF TABLES

ABBREVIATIONS:

1. AFP: Alpha-fetoprotein
2. Bcl-2: B cell Lymphoma 2
3. DNA: Deoxyribonucleic acid
4. HCG: Human chorionic gonadotropin
5. SD: Standard deviation
6. > Symbol for “greater than”

SUMMARY

Background: The uterus undergoes intense remodeling in pregnancy and subsequent involution in the postpartum period. Previous studies have demonstrated that a rise in parity affects obstetric outcomes; probably by affecting endometrial and myometrial cytoarchitecture. Parity has been shown to be protective against certain endometrial pathologies. The findings of the current study may help provide the anatomical basis for different traits noted as the parity rises.

Objective: To describe the effect of parity on the structure of uterus in pregnant rabbits

Study design: Comparative cross-sectional study.

Materials and methods: Nine rabbits**,** california white breed (*oryctolagus cuniculus*), were obtained from a private farmer. The subjects were grouped as follows; para 0 (Primigravida) rabbits in group 1, Para 1-3 (bigravida-quartigravida) in group 2, and Para >4 (>Quintigravida) in group 3. These rabbits were mated. Following mating, they were housed in a pen and were provided with a constant food and water supply. On day 18 of pregnancy, the rabbits were euthanized by injection of 20 mg/kg of phenorbarbitone. The abdominal cavity was accessed and uterus obtained en bloc. Tissue slices were obtained from different regions of the uterus by systematic sampling. These specimens were processed for paraffin embedding. The sections were stained with the Haematoxylin and Eosin stain to demonstrate general tissue architecture. Other sections were processed for immunohistochemistry for the proliferation marker, Ki-67 and anti-apoptosis protein Bcl-2. The sections were examined using a Zeiss® photomicroscope at magnification X 40 and X 100 and X 400. The endometrial gland duct density and vascular density of the myometrium and endometrium were quantified using the Image J grid system. A tool from Image J was used to obtain endometrial gland circumference as well as myometrial thickness in pixels. This was then converted to metrics. The data collected was analyzed using SPSS® version 18 for Windows® for means and variances.

Results: Endometrial gland density was noted to decrease with a rise in parity such that the percentage proportion in the primigravid rabbit was 45% compared to that of 34% and 37.5% in the bigravida-quartigravida and quintigravida groups respectively. Endometrial and myometrial vascular density increased with rise in parity. The myometrium in the primiparous was characterized by hapharzard organization of muscle fibres. In the multiparous uterus, the myometrium revealed an organization of the muscle fibres into the three layers namely; the inner submucosal zone, vascular layer and the supravascular zone. Myometrial thickness was noted to increase with parity. Ki-67 and bcl-2 showed regional variation in staining. Ki-67 stained most intensely in the endometrial glands and vascular elements. Bcl-2 stained most intensely in the endometrial lining.

Conclusion: The primigravid uterus is characterized by higher density of endometrial glands, reduced vascular density of the endometrium and myometrium, and reduced myometrial thickness. Myometrial smooth muscle layers become more organized as parity increases. This architecture of smooth muscles as parity rises, may be the reason why the multiparous uterus is efficient for fetal expulsion The higher vascularity in the higher parity group was as a result of both increased proliferation and reduced apoptosis evidenced by intense staining of the proliferation marker Ki-67 and the anti-apoptotic protein Bcl-2 in this group. The increased vascularity observed in the multiparous rabbits provides an explanation of higher likelihood of postpartum hemorrhage in the higher parity females.

CHAPTER ONE: INTRODUCTION AND LITERATURE REVIEW

1.1. INTRODUCTION

The non-gravid uterus is a thick muscular organ situated in the pelvic cavity between the urinary bladder anteriorly and the rectum posteriorly (Williams et al., 1995). During pregnancy it enlarges displacing the abdominal viscera to reach the epigastric region (Cunningham et al., 1997). Within the pelvic cavity it is held in place by peritoneal ligaments: uterosacral ligaments, cardinal ligaments and the pubocervical ligaments (Williams et al., 1995). The wall of the uterus comprises the endometrium (mucosa), myometrium (smooth muscle layer) and serosa or adventitia (Williams et al., 1995).

The endometrium comprises of an epithelium (glandular and luminal), and the underlying endometrial stroma (Williams et al., 1995). The main function of the endometrium is to support the nascent embryo via its glandular secretions (Lessey, 2000). Endometrial glands have been shown to increase in number during pregnancy and regress gradually at the end of pregnancy (Hempstock et al., 2004). Parity has been shown to be an independent prognostic factor in endometrial pathologies such as malignant mixed mesordermal tumors (Marth et al., 1997). There is evidence that grand-multiparty (5 or more pregnancies) is protective against endometrial cancer; likely as a result of the repeated protective role of progesterone (Hinkula et al., 2002). Since endometrial carcinoma has been shown to have a higher incidence in the nulliparous and low parity females, we postulated that repeated pregnancies have got an effect on the distribution of endometrial glands. Reports on the effect of parity on the endometrium are scarce.

Blood vessels within the endometrial stroma proliferate during pregnancy (Girling et al., 2007). Endometrial vasculature is important in early pregnancy as it plays a role in uterine receptivity and subsequent fetal survival (Rogers, 1996). Myometrial vascularity also increases significantly in pregnancy (Osol and Mandala, 2009). While studying rats, Skurupiy et al., (2010) demonstrated that the vascularity of the uterus diminishes with increasing pregnancies. Blood vessels in the uterus have been demonstrated to change structurally with a rise in parity (Moreira et al., 2008), suggesting that parity does have an effect on uterine vascularity. Moreira et al., (2008), found that higher parity resulted in more collagen deposition, elastosis and disorganization of the vascular wall. It is, however, not known whether parity has an effect on the vascular density of the endometrium and myometrium.

The myometrium consists predominantly of smooth muscle cells but also contains fibroblasts, blood and lymphatic vessels, immune cells and connective tissue (Williams et al., 1995). Ultrasonic studies have shown that myometrial thickness increases in all parts of the uterus, more so at the placental site and the fundus during the first and second trimesters (Degani et al., 1998, Celeste et al., 2008). Grand multiparity is one of the common etiologic factors of uterine rupture in unscarred uteri (Golan et al.,

1980), which may be as a result of thinner myometrial thickness in these muliparous females. Further, uterine volume has been shown to correlate positively with parity (Olayemi et al., 2002), probably due to thinning out of the myometrium. Ultrasonic or anatomic studies showing the effect of parity on myometrial thickness are scarce.

Proliferation, differentiation and apoptosis are processes by which the uterus maintains its homeostasis to prepare for pregnancy and to accommodate the growing fetus (Shynlova et al., 2006). Whereas cellular proliferation is augmented, apoptosis is halted in order to maintain the gravid uterus in a relatively quiescent state, a process governed by production of various anti-apoptotic proteins (Jeyasuria et al., 2011). In the rat endometrium, epithelial and stromal cells have been shown to undergo extensive proliferation in pregnancy (Goodger and Rogers, 1993). Myocytes hypertrophy and proliferate in pregnancy followed by their destruction in the postpartum period (Skurupiy et al., 2010). According to the latter, subsequent pregnancies result in increased intensity of the myocyte proliferation. In literature, studies exploring the effect of parity on proliferation and apoptosis of the gravid uterus are rare. There is evidence that parity does have an influence on the proliferation pathway of other estrogen/progesterone sensitive cells such as those found in the mammary gland (Meier-Abt et al., 2013).

After parturition, the uterus undergoes postpartum involution, which is governed by hormonal withdrawal (Lobel and Deane, 1962). Uterine involution allows the post partum uterus to return to a state capable of supporting another conceptus (Kiracoffe, 1980). An ultrasonic study done in humans indicated that uterine involution is affected by parity (Negishi et al., 1999). Indeed uterine volume in non gravid females has been shown to correlate positively with parity (Olayemi et al., 2002, Benacerraf et al., 2010). The uterus of an adult nulliparous female measures 6-8cm in length and weighs 50-70 g compared to a length of 9-10 cm and a weight of 80 g in multiparous females (Langlois, 1970). Whereas postpartum involution ensures resumption of reproductive capacity; some changes may be retained as evidenced by the differing obstetric characteristics and ultrasonic uterine dimensions with rise in parity. These obstetric characteristics include increased uterine rupture (Golan et al., 1980) and higher risk of placenta abruption (Ananth et al., 1996) as well as exercising caution when administering syntocinon for labour augmentation in multiparous females (Dawood et al., 1974). It is also known that a parous uterus requires significantly less effort to effect normal vaginal delivery than its nulliparous counterpart (Arulkumaran et al., 1984). The anatomical basis for these observations has not been elucidated. Data on the anatomical changes with parity are useful to inform intervention strategies to mitigate the poor obstetric outcomes. This study was therefore undertaken to elucidate how parity affects the distribution of endometrial glands, vascularity of the endometrium and myometrium as well as its influence on proliferation and apoptosis in these layers.

1.2. LITERATURE REVIEW

1.2.1. GENERAL FEATURES

The uterus is the major female reproductive organ of most mammals, whose main function is to support a fertilized ovum. It is a hollow organ that opens at one end at the oviducts and terminates on the other end in the cervix and vagina (Williams et al., 1999). Four main types of uteri have been reported to occur among the different mammalian orders based largely on differences in the prominence of the body and the two horns. The simplex type is seen in primates, has no horns, duplex type as in rodents and rabbits, these have large horns as well as 2 cervices (Akinloye and Oke, 2010) and the bicornuate type present in ruminants and pigs, which have uterine horns and a body terminating on one cervix (Hafez, 1970).

The adult human uterus is a pear shaped organ that weighs 40-70 g and measures 7-8 cm long in non-pregnant, nulliparous females (Cunningham et al., 1997), whereas in parous females it averages 80 g or more (Langlois, 1970). It is situated in pelvic cavity between the bladder anteriorly and the rectum posteriorly (Williams et al., 1997). Microscopically, it comprises the endometrium; an inner mucosal lining, which provides the environment for foetal development, the myometrium, which makes up the bulk of the uterus, and the parametrium.

During pregnancy, the uterus undergoes profound tissue remodeling, increasing in both capacity and weight. It is consequently transformed into a relatively thin-walled muscular organ of sufficient capacity to accommodate the fetus, placenta, and amniotic fluid. By the end of pregnancy the uterine capacity is 500 to 1000 times greater than in the non-pregnant state (Cunningham et al., 1997). The structural changes responsible for this occur mainly in the myometrium (Cunningham et al., 1997). The endometrium also undergoes benign proliferative changes in pregnancy on account of higher progesterone levels (Groothius et al., 2007). These changes are discussed below.

1.2.2. ENDOMETRIAL GLAND DUCT DENSITY AND SIZE

The endometrium is vital for normal fertility in all mammals. It comprises of a luminal epithelium, glandular epithelium and the underlying endometrial stroma (Williams et al., 1995). Found within the endometrial stroma are blood vessels, nerves, immune cells as well as endometrial glands. The endometrial glands are tubular; they run perpendicular to the luminal surface and penetrate the myometrial layer. In mammals, endometrial histology varies throughout the menstrual cycle and is influenced by estradiol and progesterone (Cunningham et al., 1997). Estradiol induces proliferation of the basalis and functionalis endometrial layers and progesterone promotes glandular development and secretion, and initiates the necessary changes for allowing embryonic implantation to take place. Progesterone is therefore responsible for converting the estrogen primed endometrium into a receptive state suitable to support pregnancy (Groothius et al., 2007). The Arias Stella reaction is a benign,

proliferative change that occurs in the uterine epithelium in response to an increase in progesterone levels as is seen in pregnancy (Arias-Stella 1954). It is characterized by intraluminal budding, nuclear enlargement and hyperchromatism, cytoplasmic swellings and vacuoles.

All mammalian uteri contain straight tubular endometrial glands, which secrete and transport substances that are essential for the survival and development of the conceptus (Gray et al., 2002). Uterine secretions are particularly important for the nourishment in the early stages of pregnancy, before establishment of the hemotrophic nutrition by the placenta (Gray et al., 2001b, Hempstock et al., 2004). In sheep, endometrial gland density has been shown to be directly related to survival and development of the conceptus (Gray et al., 2001a). Morphologically the endometrial glands are said to be best developed and most active during early pregnancy (Hempstock et al., 2004). The glands then gradually regress over the late phases of pregnancy. Factors that have been shown to affect endometrial gland density include dietary supplements, gestational age as well as hormones (Amira et al., 2011). In non-pregnant human females, progesterone, both endogenous and synthetic, is reported to inhibit endometrial glandular proliferation in premenopausal females (Moyer and Felix, 1998). Deligdisch (1993) demonstrated that the histologic effects of the steroid sex hormones on the endometrium depend on the hormone type, potency, dosage and the host receptor status.

Following parturition, the endometrium has the capacity to repair and regenerate (O'shea and Wright, 1984). Huang et al., (2012) described a parturition induced repair of the endometrium characterized by stromal-epithelial transition. According to these authors, there exists a subpopulation of stromal cells that are capable of differentiating into glandular or luminal epithelial cells (Huang et al., 2012). Uterine glands undergo gradual regression in the postpartum period (Krajničáková et al., 1999). Reports on the effect of parity on the endometrium are scarce. However, parity has been shown to be an independent prognostic factor in endometrial pathologies such as malignant mixed mesordermal tumors (Marth et al., 1997). There is evidence that grand-multiparty is protective against endometrial cancer; likely as a result of the repeated protective role of progesterone (Hinkula et al., 2002).

1.2.3. VASCULAR DENSITY OF THE ENDOMETRIAL STROMA AND THE MYOMETRIUM

The human uterus has an anastomotic blood supply arising from uterine, ovarian and vaginal arteries (Ramsey, 1994). Bilateral uterine arteries penetrate the myometrium and give rise to the circumferential arcuate arteries (Farrer-Brown *et al*., 1970). These in turn branch to form the radial arteries, which traverse the myometrium and perforate the endometrium as small calibre conductance vessels, known as spiral arterioles. Blood supply to the endometrium arrives through the radial arteries, which arise from the arcuate arteries within the myometrium. After passing through the

myometrial–endometrial junction the radial arteries split, to form the smaller basal arteries that supply the basal portion of the endometrium and the spiral arterioles, which continue towards the endometrial surface.

Sufficient uteroplacental blood flow is essential for normal pregnancy outcome and is accomplished by coordinated growth and remodeling of the entire uterine circulation in addition to a new fetal vascular origin; the placenta (Osol and Mandala, 2009). During pregnancy, the diameter of the uterine artery approximately doubles its size (Palmer et al 1992). This enlargement in arterial caliber occurs more often with little or no thickening of the vascular wall (Osol and Mandala, 2009). Smaller arcuate and radial arteries remodel in a similar pattern, with documented enlargements in luminal diameter ranging from 25-220% with no change or increase in thickness (Moll et al., 1983). There is documentation of dilation of uterine vascular beds in pregnant rabbits (Sullivan and Tucker, 1975).

In humans, the spiral arterioles, which supply the functional layer of the endometrium, have a distinctive coiled appearance that becomes more pronounced during the secretory phase of the menstrual cycle (Rogers, 1996). Each spiral arteriole provides blood to a uterine luminal surface area estimated at 4–9 mm^2 (Bartelmez, 1933), with little or no overlap between areas. Capillaries branch from the spiral arterioles at all levels supplying the stroma and periglandular networks. Just below the endometrial surface the spiral arterioles break up into the prominent subepithelial capillary plexus. This plexus drains into a number of venules that pass down through the endometrium, collecting blood from other capillaries on the way. The numerous venules join to form veins, which pass out of the endometrium into the myometrium (Rogers, 1996).

The endometrial stroma is composed of endometrial stromal cells and vessels of which the spiral arteries predominate. Other components include stromal granulocytes and stromal foamy cells. These stromal components proliferate, differentiate and disintegrate throughout the reproductive cycle in response to steroid hormones (Maksem et al., 2007). Progesterone has been reported to decrease gland to stroma ratio (Wheeler et al., 2007). Some of the other changes that have been noted to occur in the endometrial stroma include; a predominance of stromal granulocytes (Pace et al., 1989), increase in thickness and branching of the stromal vessels (Hafez and Tsutsumi, 1966). The two main mechanisms of endometrial vessel formation include intussusception and sprouting (Weston and Rogers, 2000). The former consists of internal division or splitting of pre-existent vessels. In the latter, endothelial cell activation, degradation of basement membrane, migration and proliferation lead to formation of tubules, stabilization of pericytes, and extracellular matrix formation (Makanya et al., 2009).

The capillary density of non pregnant sows has been shown to vary during the different stages of the estrous cycle (Kaeoket et al., 2002). In fact, the vascular density of the uterine mucosa in ewes exhibits a 2-fold increase (Reynolds and Redmer, 1992). Some authors have also demonstrated that the vascular density of endometrial tissues increases gradually throughout the gestation period (Parry, 1950, Reynolds and Redmer, 2001). In pregnant mares, endometrial maternal capillaries have been shown to have an ongoing supply of angiogenic and vasculogenic factors throughout pregnancy to ensure continuing development of maternal capillary networks (Allen et al., 2007). In addition to increased vascular density, endometrial vessels become more permeable in pregnancy (Keys and King, 1988).

The myometrial vascular channels established during pregnancy diminish during postpartum involution (Skurupiy et al., 2010). It is known that abnormal uterine blood vessels and angiogenic factors are part of the theories to the pathophysiology of myoma formation (Stewart, 2001). It is also known that parity reduces uterine myomas, an observation which may be related to a reduction in endometrial vascularity. If this concept is verified, follow up studies can check whether myometrial healing is slower in multiparous females following caesarean section.

1.2.4. MYOMETRIAL SMOOTH MUSCLE ORGANIZATION AND MYOMETRIAL THICKNESS

The myometrium is the middle layer of the uterine wall consisting mainly of smooth muscle cells as well as supporting connective tissue, immune cells, vascular tissue and lymphatic tissue (Williams et al., 1999). The myometrium is organized into three layers; the inner and outer layers mainly composed of smooth muscle disposed circularly and longitudinally respectively and an intermediate layer which has hapharzard/criss-crossing smooth muscle fibers which act as ligatures during involution after parturition to prevent blood loss (Brown et al., 1991, Cavaillé et al., 1996, Williams et al., 1999). The smooth muscle in the inner and outer layer are compact with little extracellular matrix while the intermediate layer has an abundance of interposed blood vessels (Brown et al., 1991).

The main function of uterine smooth muscle is to remain quiescent during fetal development, then to contract at term to expel the fetus (Cunninghams et al., 1999). Bundles of smooth muscle within the myometrium are anchored by a connective tissue framework that also allows for uterine distention during pregnancy (Rehman et al., 2003). Myometrial immune cells have been noted to increase in number towards the end of pregnancy and are thought to be involved in labour activation and postpartum involution of the uterus (Shynlova et al., 2013). Unlike other smooth muscle, the myometrium is largely under hormonal control (Hertelendy and Zakar, 2004). Hormones such as estrogen and progesterone promote its growth and ensure its quiescence during gestation, while

hormones such as oxytocin, prostaglandins and nitric acid control its contractility (Hertelendy and Zakar, 2004).

The myometrium is the main component of uterine enlargement during pregnancy (Cunninghams et al., 1997). Although uterine growth during the first few weeks of pregnancy is accomplished by increased numbers of smooth muscle cells, i.e., hyperplasia, and a small contribution from increased cell size, hypertrophy, the predominant growth of the uterus during pregnancy is by stretch induced myometrial hypertrophy (Ramsey, 1994). This myometrial transformation that occurs during pregnancy is said to be different in the various parts of the uterus because of specialized functional load in the different parts (Dolgikh et al., 2012). Ultrasonic studies have shown that myometrial thickness increases in all parts of the uterus, more so at the placental site and the fundus during the first and second trimesters (Degani et al., 1998, Celeste et al., 2008). The greater fundal thickness is proposed to increase the efficiency of fundal dominance during labor (Buhmischi et al., 2003). It has also been shown that the myometrial thickness at the fundus can be used as a predictor of successful external cephalic version (Buhimschi et al., 2011). In humans, the upper uterine segment has more contractile phenotypes of smooth muscle to push down the baby and initiate delivery while the lower uterine maintains a more relaxed phenotype to facilitate delivery of the baby (Lye et al., 1998).

The thickness of the lower uterine segment has been used as a predictor of uterine rupture in scarred uteri (Qureshi et al., 1997). Grand multiparity is one of the common etiologic factors of uterine rupture in unscarred uteri (Golan et al., 1980), which may be as a result of thinner myometrial thickness in these muliparous females. In the third trimester however, the lower uterine segment remarkably reduces in thickness (Degani et al., 1998). Grand multiparity is one of the common etiologic factors of uterine rupture in unscarred uteri (Golan et al., 1980), which may be as a result of thinner myometrial thickness in these muliparous females. Further, uterine volume has been shown to correlate positively with parity (Olayemi et al., 2002), probably due to thinning out of the myometrium.

Parameters that are known to affect myometrial thickness in pregnancy include; site of placental attachment (Degani et al., 1998), diabetes (Favaro et al., 2010), part of the uterus in humans, the lower uterine gradually reduces in thickness (Degani et al., 1998). Studying the uterus of pregnant mice, Favaro et al., (2010), established that prolonged uncontrolled diabetes significantly reduces myometrial thickness: the myometrial thickness being 152.3 $\pm$ 2.35 μm in the control group and 71.22 $\pm$ 2.35 μm. Through extensive search of literature there are no ultrasonic or anatomic studies showing the effect of parity on myometrial thickness.

1.2.5. CELL PROLIFERATION AND APOPTOSIS IN THE ENDOMETRIUM AND MYOMETRIUM

During pregnancy the human uterus undergoes increase in volume and weight, mostly as a result of myometrial remodeling, where both hypertrophy and hyperplasia are evident (Ono et al., 2008). Uterine cell proliferation in early pregnancy is mediated by locally produced growth factors many of which are under the influence of progesterone (Graham and Clarke, 1997, Ogle et al., 1999). Androgen receptors found in uterine cells are highly expressed in the proliferative stage of pregnancy and are known to be central in regulation of cellular proliferation (Liu et al., 2013). Oestrogen has also been known to be key in the up-regulation of markers of proliferation such as Ki-67 and Bcl-2 in the receptive endometrium (Shao et al., 2013).

The expression of Ki-67 protein is strictly associated with cell proliferation (Scholzen and Gerdes, 2000). It is an excellent marker for determining proliferation given that it is expressed in cells during the active phases of the cell cycle (G1, S, G2) and is absent in the resting phase, G0 (Scholzen and Gerdes, 2000). On the other hand, Bcl-2 and related cytoplasmic proteins are key regulators of apoptosis and therefore promote cellular survival (Adams and Cory, 1998). Apoptosis is an essential physiological process for selective elimination of cells. Apoptosis is driven by a family of caspases, which are regulated by Bcl-2 (Tsujimoto, 2000). The Bcl-2 and related proteins comprises of both anti-apoptotic and pro-apoptotic members of which Bcl-2 and Bcl-XL are anti-apoptotic.

The pre-ovulatory endometrium in humans is highly proliferative and expresses high amounts of proliferative markers such as Ki-67, while the post-ovulatory endometrium hardly stains for proliferative proteins (Ferenczy and Mutter, 2008). The equine endometrium undergoes cellular proliferation throughout the reproductive cycle (Gerstenberg et al., 1999). During pregnancy in mares, all endometrial layers have been found to be Ki-67 positive (Silva et al., 2011). It is also known that the non-gravid human endometrium undergoes cyclical apoptosis (Otsuki, 2001). Decreased expression of the anti-apoptotic marker Bcl-2 during the secretory phase of the endometrium is consistent with the appearance of anti-apoptotic cells during the same phase (Grompel et al., 1994, Otsuki, 2001).

The myometrium also undergoes repeated cycles of cellular proliferation and degeneration in response to hormonal signals during a normal mammalian reproductive life span. In humans, the proliferation marker Ki-67 has been found to be higher in myocytes during the luteal phase (Suzuki et al., 2012). Uterine growth in the first weeks of pregnancy is accomplished mainly by hyperplasia with a smaller contribution from hypertrophy in both humans (Ramsey, 1994), and rats (Shynlova et al.,

2006). During this early phase of myocyte hyperplasia, there is a concomitant increase in anti-apoptotic markers (Shynlova et al., 2006).

The number of muscle cells in the human uterus at term is estimated at 200 billion, each minute fusiform cell measuring about 5–10 μm in diameter and about 200 μm in length (Tabb et al., 1991). The origin of the new smooth muscle cells is unclear, they may arise from existing smooth muscle cells or they may be a product of smooth muscle differentiation (Ono et al., 2008). It has been hypothesized that there may be adult myometrial stem cells responsible for myometrial hyperplasia (Maruyama et al., 2010).

1.3. JUSTIFICATION OF THE STUDY

The relationship between parity and pregnancy complications continues to be of interest to obstetricians (Bai et al., 2002). Parity is defined as the number of times a female has given birth to a viable fetus and not the number of fetuses delivered (Cunningham et al., 1997). Multiparity and maternal mortality are closely related since with each successive pregnancy females are repeatedly exposed to the complications of labour and gravidity (Begum 2003). Pregnancy in the multiparae has been considered risky for many decades (Solomons, 1934). Linear association has been found between parity and adverse maternal and neonatal outcomes such as malpresentation, labour dystocia, postpartum hemorrhage, placentation abnormalities and the need for caesarian section (Shechter et al., 2010). Uterine rupture is one of the most appalling obstetric emergencies (Bujold and Gauthier 2002). On the contrary, other studies have shown that women with a high parity with no previous complicated pregnancy have a low risk of obstetric complications (Majoko et al., 2004, Yasmeen et al., 2010). There are reports that a parous uterus requires less effort to significantly expel the fetus in normal vaginal delivery than is nulliparous counterpart (Arulkumaran et al., 1984). In addition, parity is believed to be protective from uterine fibroids (Baird and Dunson., 2003) and endometrial cancer (Albrektesen, 2009). This study sets out to provide an anatomical explanation to these differing obstetric features as a result of parity.

1.4. STUDY QUESTION

What are the differences of the structure of the uterus with increasing parity in pregnant rabbits?

1.4.1. GENERAL OBJECTIVE

To determine the effect of parity on 3rd trimester uterine structure in rabbits.

1.4.2. SPECIFIC OBJECTIVES

To determine whether the following uterine features are affected by parity

1. Endometrial gland density and size
2. Vascular density of the endometrial stroma and the myometrium.
3. Myometrial smooth muscle organization and myometrial thickness.
4. Proliferation and apoptosis within the endometrium and myometrium.

CHAPTER TWO: MATERIALS AND METHODS

2.1. EXPERIMENTAL ANIMALS

Use of experimental animals is acceptable as long as the benefits of the proposed study outweigh the suffering of the animal (Baumans, 2004). Rabbits maintain pregnancy up to 28 days. Their short gestation span and their similarities to humans in placentation make the rabbits a suitable study model for investigating uterine remodeling. The rabbits, California white rabbits (O*ryctolagus cuniculus*) were obtained from a private farmer. The rabbits used in the study were grouped as described in table 1 below. The rabbits were mated. The existence of a copulation plug in the vagina of the rabbits was used as evidence of successful mating. In the laboratory the rabbits were kept in pens floored with saw dust. They were fed on commercial rabbit pellets, half a cup of pellets per 5 kilogram body weight daily. They were also supplied with a steady supply of fresh water.

2.1.1. ETHICAL CONSIDERATIONS

Ethical approval was obtained from the Animal Use and Welfare Committee of the University of Nairobi.

2.1.2. SAMPLE SIZE

This is a descriptive comparative study that compared means of continuous data amongst the 3 groups to be studied. For this reason, the formula below was used, appropriate for such a study, as described by Eng (2003);

$$N = \frac{4\sigma^2 (Z_{crit}+Z_{pwr})}{D^2}$$

Where N is the desired total sample size, σ is the SD (standard deviation of each group), D is the smallest meaningful difference and Z_{crit} and Z_{pwr} are constants determined by the specified significance criterion (for our case 0.05) and the desired statistical power (0.8 for this study) respectively. With the above assumptions from previous workers studying similar parameters (myometrial thickness), where D was 2.1 mm, and σ was 2.5 mm the calculated sample size was found to be 3 rabbits per group and a total of 9.

2.1.3. SELECTION CRITERIA

Pregnant rabbits within the third trimester were placed into three groups as illustrated in the table below:

Table 1: Grouping of the rabbits

Group	Parity of the rabbits
1	Primigravida
2	Bigravida-Quartigravida
3	> Quintigravida

Each group utilized 3 rabbits. Rabbits that qualified to be in any of the above groups were selected by the simple random method. For example, if there were 5 rabbits that met the inclusion criteria specified below; those rabbits were given numbers and thereafter selected using the Excel computer program to randomly generate numbers. These rabbits were within 3 months of age of each other. Rabbits with known systemic comorbidities, previous surgery or those on therapeutic medication were excluded from this study. The nulliparous, non-pregnant rabbit was excluded as the study sought to decipher the changes of the uterus resulting from parity with all the rabbits in the same uterine state (pregnancy).

2.1.4. WEIGHING THE RABBITS, ANAESTHESIA AND DISSECTION

On day 18 after mating, the pregnant rabbits were moved from their pen. Their weight was taken using a kitchen scale. They were then euthanized with an overdose of phenobarbitone (20 mg/kg), through intravenous infusion. The abdominopelvic cavity was accessed via a ventromedian incision. The anterior abdominal wall was retracted laterally to gain access into the pelvic cavity. The uterus was harvested en bloc, separated from the other reproductive organs and its weight obtained using a kitchen scale. The weighing of all the rabbit and the uterus were done with the liters in situ.

2.1.5. TISSUE SAMPLING

Once obtained, the uterus was divided into ten approximately equal portions numbered 1-10 as shown by the black lines in the diagram below (Fig.1). The parts obtained closest to the fallopian tube were put in one place, the parts from the mid-cornual regions in another as well as for the cervical regions. Each of these parts as described, from each animal, were bunched together and the lottery method used to obtain a sample to undergo histological processing. The number that had been given to the sample prior to bundling them up could be used to trace back specimens to the specific animal.

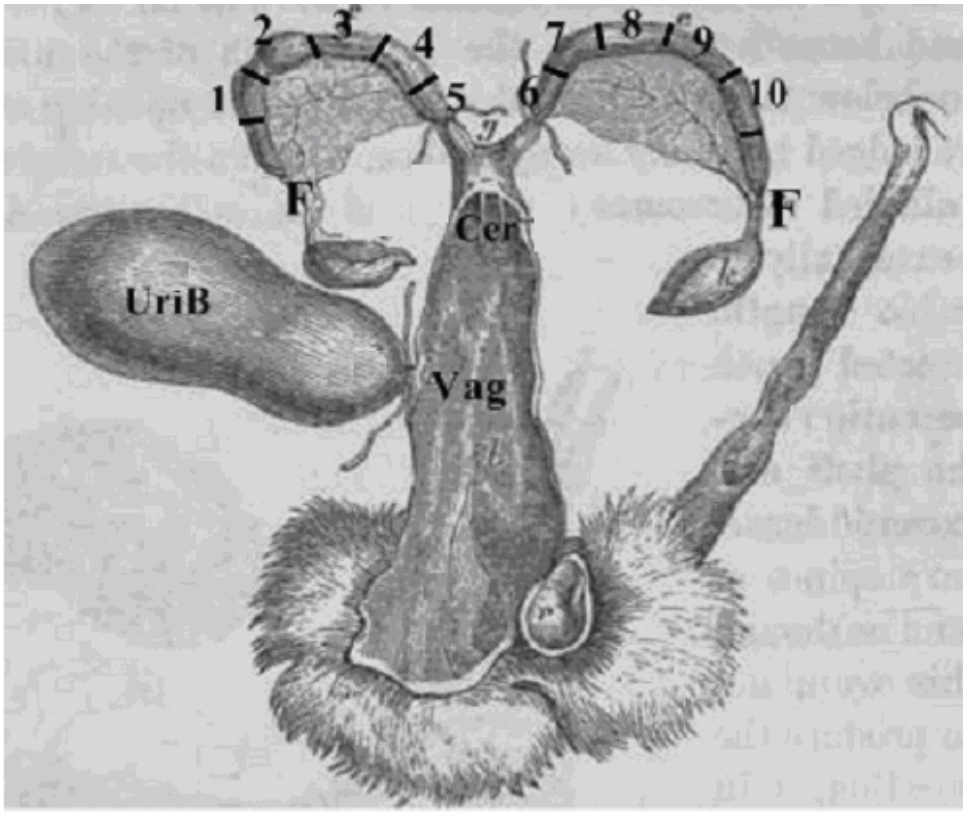

Figure 1: Diagram of the internal genitalia of a rabbit showing some of the pelvic organs including the uterus.

This diagram was adapted from Jones (2013). It shows how sampling of the uterus was carried out as represented by the numbers 1-10. 'F' is the fallopian tube, 'UriB' is the urinary bladder 'Vag' is the vagina and 'Cer' represents the cervix.

The regions of the bicornuate uterus of these rabbits studied included the following; central region of one of the cornua, part of the uterus bordering to the fallopian tube and the cervix. Specimens picked from the placental site were discarded.

2.2. PROCESSING FOR LIGHT MICROSCOPY

Fixation of the specimens for microscopy was done using 10% formaldehyde solution. 5mm samples were obtained from the fixed specimens. These underwent dehydration through increasing concentrations of ethanol 1 hour in each (70%, 80%, 90%, 95%, 100%) and clearing in xylene (2 stations 30 minutes each). Infiltration and embedding were done using paraffin wax. The wax blocks were then supported on wooden blocks then cut using a base sledge microtome, floated in a water bath and left for drying in an oven, overnight. The sections were then analyzed by light microscopy after mason trichrome staining to assess myometrial vascularity as well as thickness of the myometrium as described in standard textbooks of histological techniques (Drury et al., 1967).

2.3. THE ENDOMETRIUM AND ENDOMETRIAL GLAND DENSITY AND SIZE

The specimens processed for light microscopy as described above were used to study the endometrium. The H and E stained slides were studied at X 40, X 100 and X 400. The proportion of glands/ducts within the endometrial stroma was used to represent the "density of glands/ducts." This was determined using the point intercept method by dropping a grid in ImageJ software (Fig. 2) as described by Baecker. (2010). The numbers of glands in each box of the grid were counted and the total area where the counting was done was also obtained. In each group of the pregnant rabbits the systemic random sampling was employed to select the sections to be measured. Five slides of the endometrium were selected randomly, from each section; the counting was done at 5 random points. An average was obtained for each group. The proportion of the area of the endometrium occupied by endometrial glands was presented as a percentage as follows:

$$100 \times \frac{\text{Total pixels occupied by endometrial glands}}{\text{Total pixels occupied by a given area of the endometrium}}$$

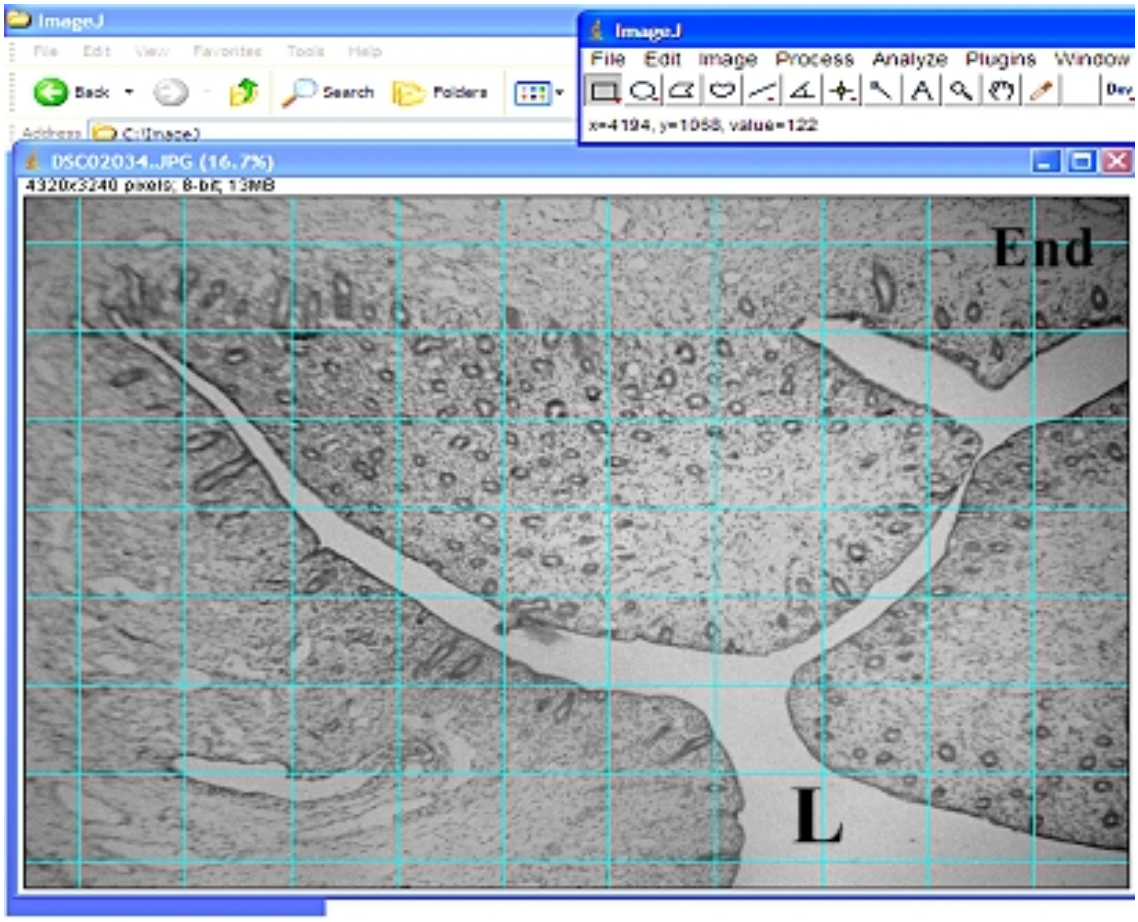

Figure 2: Illustration of how to determine endometrial gland density

A black and white photomicrograph transformed by the Image J program, with a superimposed grid from the same program. It is a section of a primiparous rabbit uterus from the mid-cornual part, stained with H and E, at X 100 magnification. The numbers of endometrial glands within each box were counted. L is the lumen of the uterus.

In each group of rabbits, the circumferences of 15 endometrial glands were measured at X400 and their average obtained per field. Five sections were studied per group. This was done using the program Image J. A tool on this program measured the circumference of the glands in pixels. The flexible tool was taken round the inner circumference of a gland and the measurement obtained was recorded in pixels. The equivalent of 1mm in pixels was done by marking a distance of 1mm between two points on a piece of paper that was mounted on a slide. This slide was examined at X400 and photographed. The distance between these two points was used to calibrate the grid of image J to give its equivalent in pixels. The images were converted to black and white and their binary form to remove color as a confounder in measuring pixels. For each groups of rabbits 15 glands were counted and an average was obtained. The figure was then converted from pixels to millimeters.

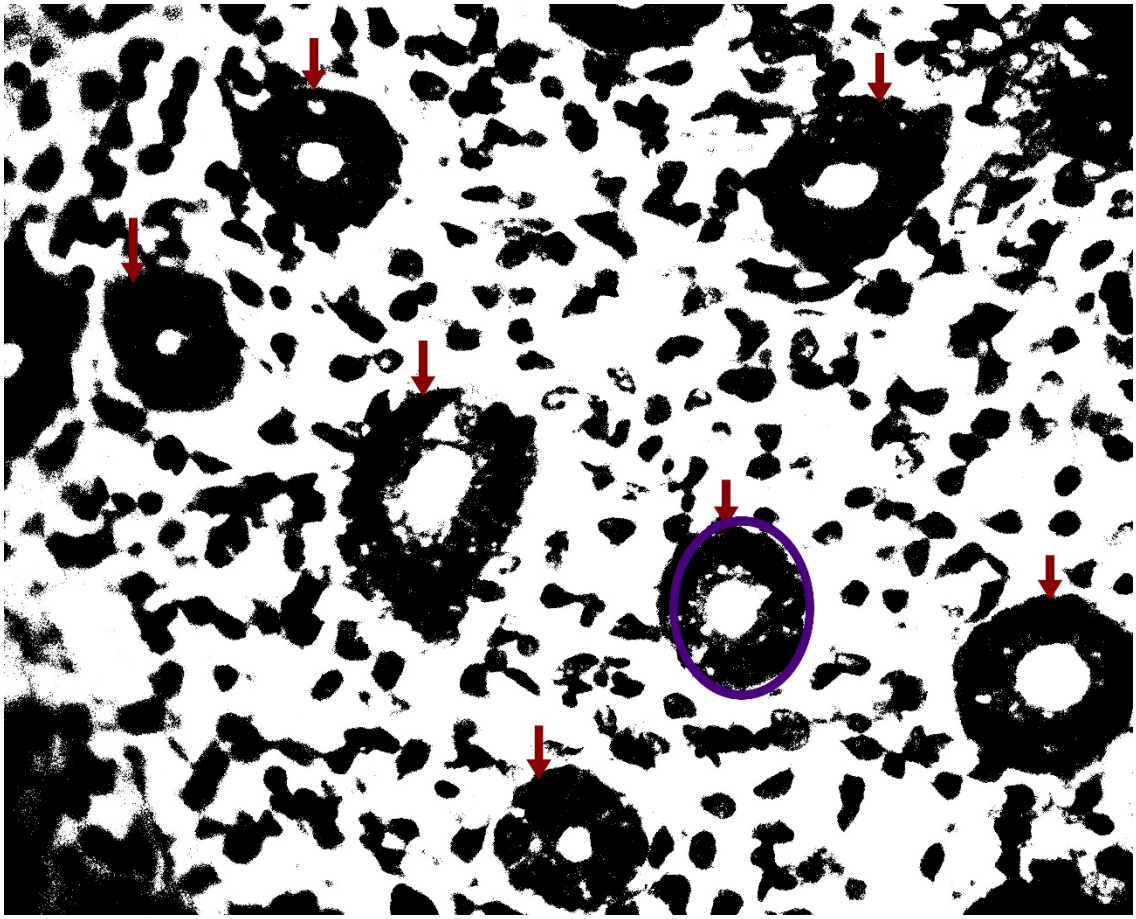

Figure 3: Illustration of how to determine endometrial gland size

A binary/black and white photomicrograph of the endometrial stroma of a primigravid uterus at X400, following H and E staining and subsequent transformation using the program image J. A tool was used to draw around the gland as shown by the purple line to get the circumference. The glands are as shown by the red arrows.

2.4. DETERMINATION OF VASCULAR DENSITY WITHIN THE ENDOMETRIAL STROMA AND THE MYOMETRIUM

Endometrial and myometrial vascular density (vascular area as a proportion of total tissue area) were determined using the point intercept method by dropping a grid from the Image J software as shown in the figure below. In each group of the pregnant rabbits, 5 sections of the endometrium were selected randomly, from each section; the counting was done at 5 random points. An average was obtained for each group. The proportion of the area of the endometrial stroma occupied by endometrial blood vessels was presented as a percentage as follows:

$$100 \times \frac{\text{Total pixels occupied by stromal vessels}}{\text{Total pixels occupied by a given area of the endometrial stroma}}$$

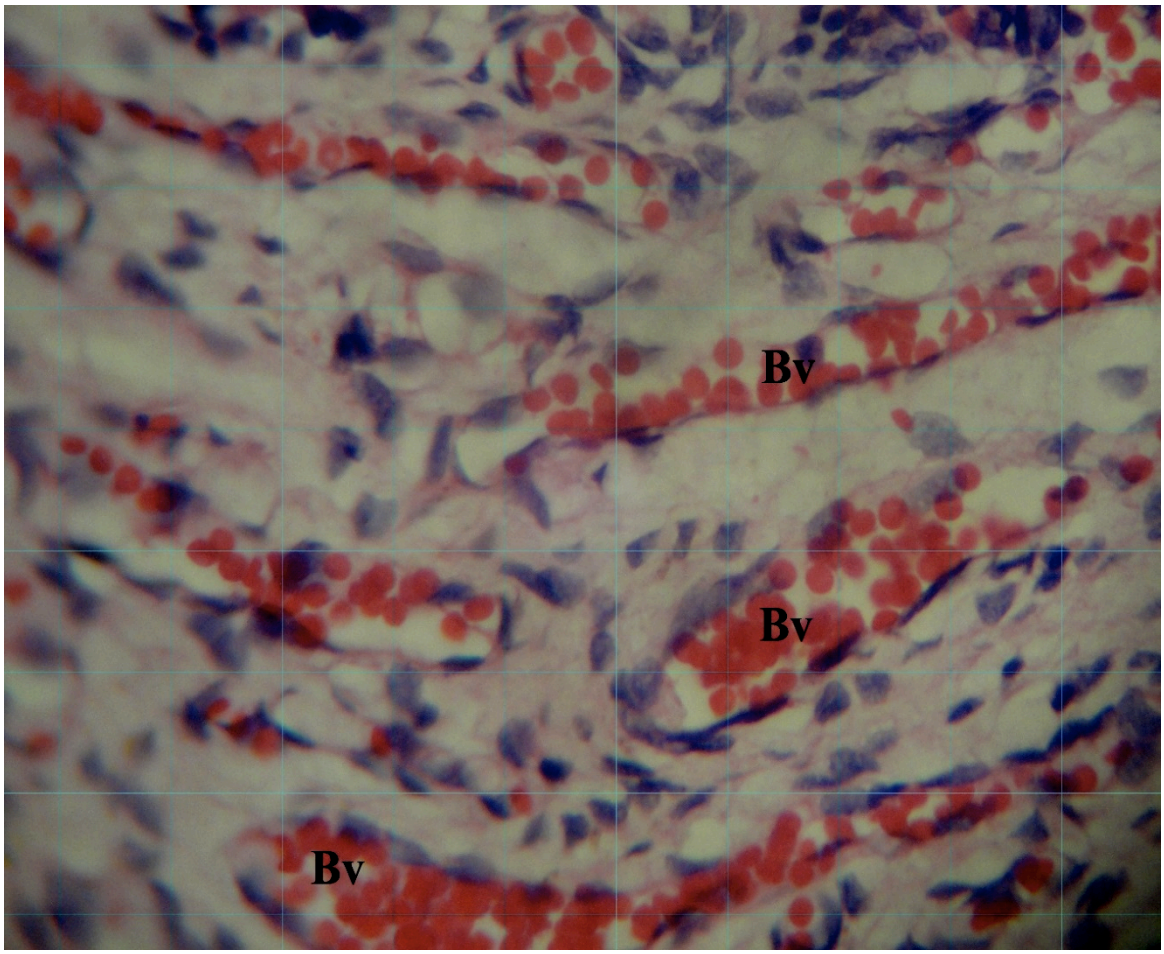

Figure 4: Determination of the vascular density of the endometrium

A photomicrograph of the endometrial stroma of a multiparous rabbit, obtained from the mid-cornual section of the uterus stained with H and E at X 400. An image J grid has been superimposed on this

photomicrograph. For the purpose of demonstration, this photograph remained colored, since the blood vessels (Bv) are more discernible.

The procedure described above for the endometrium was applied for the myometrium. In each group of the pregnant rabbits, 5 sections of the myometrium were selected randomly, from each slide, the counting was done at 5 random points. An average was obtained for each group. The proportion of the area of the myometrium occupied by blood vessels was presented as a percentage as follows:

$$100 \times \frac{\text{Total pixels occupied by myometrial blood vessels}}{\text{Total pixels occupied by a given area the of myometrium}}$$

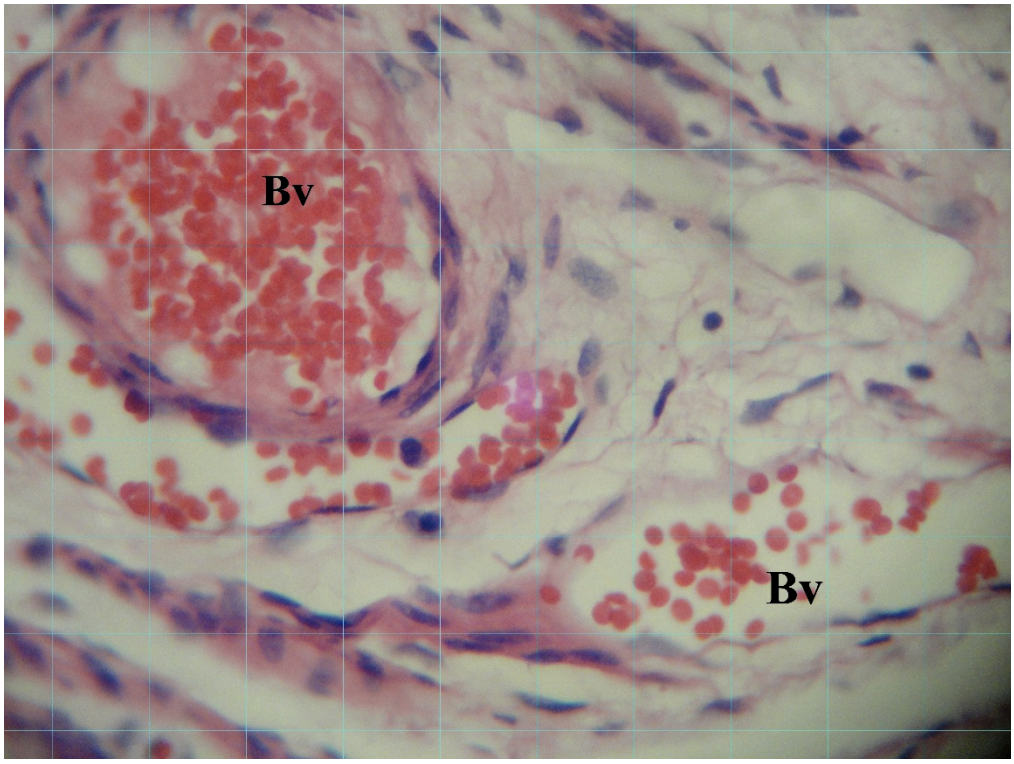

Figure 5: Determination of vascular density within the myometrium

Photomicrograph of the vascular zone of the myometrium of a multiparous uterus at X400, H and E stain. An Image J grid has been superimposed. The number of times the blood vessels (Bv) fell on the intersect were counted as well as the entire field of the grid

2.5. MYOMETRIAL MORPHOMETRY

The sections prepared were assessed for myometrial muscle fiber disposition and myometrial thickness. The myometrial thickness was expressed as a proportion of the entire wall as well as the average thickness of the myometrium in the sections studied for each group. This was done using a tool on the program Image J. Image J processed the length in pixels. The equivalent of 1mm in pixels was done by marking a distance of 1mm between two points on a piece of paper that was mounted on a slide. This slide was examined at X40 and photographed. The distance between these two points was used to calibrate the grid of image J to give its equivalent in pixels. The average myometrial length in each group was then converted to mm.

The proportion of the junction wall occupied by the myometrium (Fig. 6) was determined by:

$$100 \times \frac{\text{Thickness of myometrium (a) /pixels}}{\text{Thickness of the myometrial wall (b) /pixels}}$$

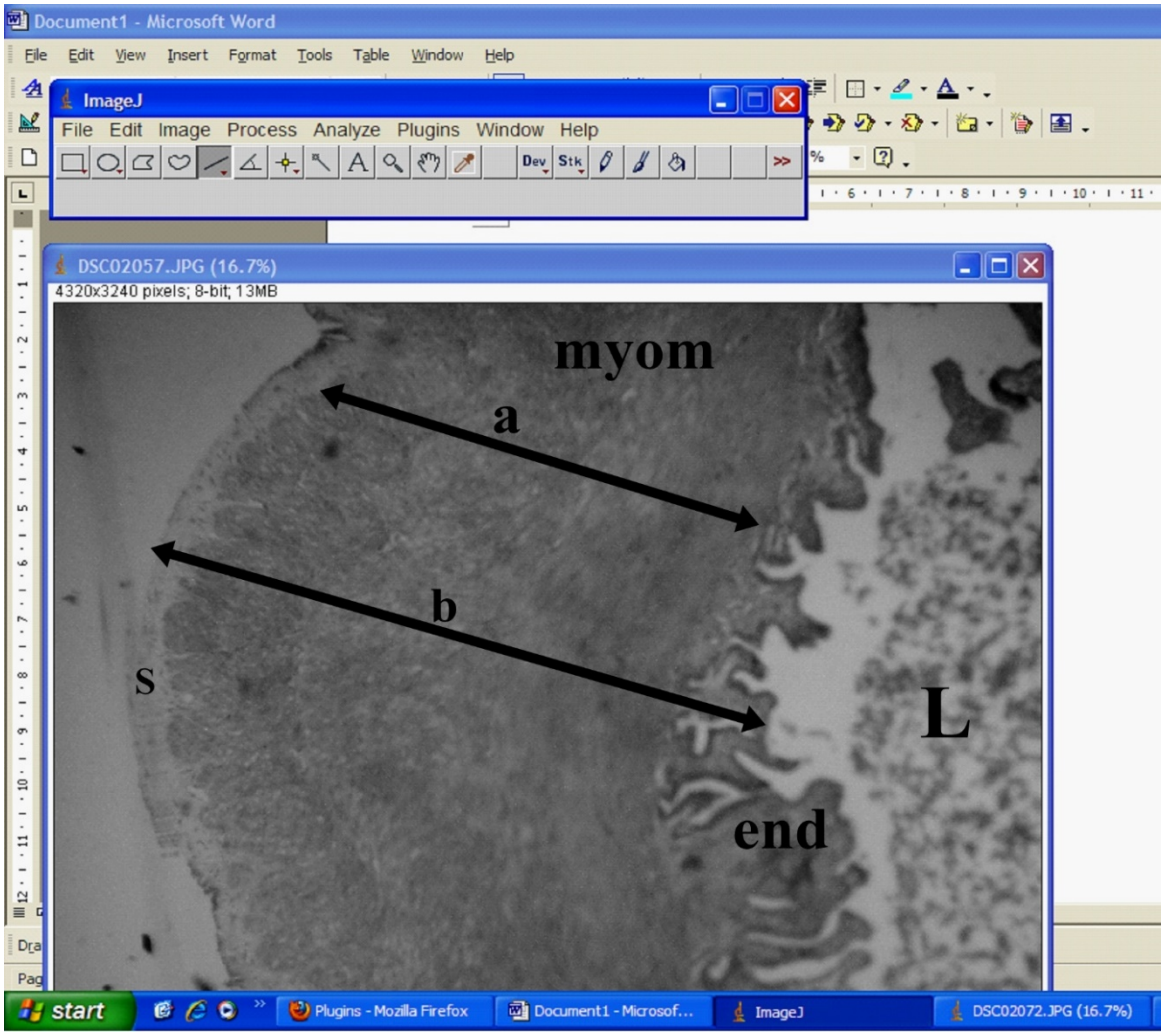

Figure 6: Determination of myometrial thickness

A photomicrograph of a group 2 rabbit (biparous-quadriparous) at X40, H and E staining in the black and white form, as transformed by Image J for the purpose of measurement. L is the lumen, End the endometrium. The lines “a” and “b” measured the myometrial and the entire thickness of the uterus respectively.

2.6. IMMUNOHISTOCHEMISTRY FOR PROLIFERATION AND ANTI-APOPTOSIS MARKERS

The standard protocol for immunohistochemistry was carried out for apoptosis regulatory protein, Bcl-2, which is an anti-apoptotic protein, (Adams and Cory 1998) and an endogenous marker for proliferation and Ki-67 (Scholzen and Gerdes 2000). Monoclonal antibodies against these two antigens were used. Tissue sections obtained from the uterus of the rabbit via simple random sampling were taken through microwave fixation in paraffin, deparaffinized in xylene three times, and rehydrated through a graded ethanol series from 99.5 to 60%. After quenching the intrinsic peroxidase

activity by immersing the sections in 0.3% (vol/vol) hydrogen peroxide containing 0.1% (wt/vol) sodium azide for 30 min, the sections were incubated with 10% (vol/vol) normal rabbit serum for 30 min. The primary antibody were applied to the sections respectively and incubated overnight at 4° C in a moist chamber. After washing with 10 mM PBS, the primary antibody was detected and visualized by means of biotinylated secondary antibody-streptavidin peroxidase using a Histofine according to the manufacturer's instructions.

2.7. STATISTICAL ANALYSIS AND DATA PRESENTATION

Morphometric data were entered into SPSS software (Version 17.0, Chicago Illinois) for statistical analysis. Means and standard deviations for these morphometric measurements were calculated and standardized with the weight of the uterus. The Fisher's exact test was used to test statistical significance of the data obtained in the different parity groups and the chi square to compare proportions.

CHAPTER 3: RESULTS

3.1 GENERAL FINDINGS

Nine rabbits met the inclusion criteria and were categorized into the 3 groups described above. The rabbits had an average liter size of 7. The body mass of the rabbits and the weight of the uteri are as shown in tables 2 and 3 respectively. The average weight of the uterus was observed to increase in size (P=0.58), not statistically significant. The body-mass normalized uterine weight was obtained by dividing the weight of the uterus by the mass of the rabbits. This parameter was noted to increase with parity but it was not statistically significant (P=0.09). The results are as shown in table 4.

Table 2: Body mass of the rabbits.

Variable	Primigravida (Weight in grams)	Bigravida-Quartigravida (Weight in grams)	Quintigravida (Weight in grams)
Animal 1	1330.40	1978.00	2509.80
Animal 2	1270.50	2000.80	2879.50
Animal 3	2102.70	2403.05	1509.50
Mean	1939.40± 590.64	2050.27± 805.63	2005.23± 454.89

Table 3: Weight of the uterus of the rabbits used in the study.

Variable	Primigravida (Weight of the uterus grams)	Bigravida-Quartigravida (Weight of the uterus grams)	Quintigravida (Weight of the uterus in grams)
Animal 1	40.10	41.15	53.10
Animal 2	38.75	45.15	43.40
Animal 3	50.90	55.01	49.40
Mean	43.25± 6.65	47.10± 7.13	48.63± 4.89

Table 4: Body mass-normalized uterine weight

Variable	Primigravida (Body mass normalized uterine weight, g/g)	Bigravida-Quartigravida (Body mass normalized uterine weight, g/g)	Quintigravida (Body mass normalized uterine weight, g/g)
Animal 1	0.0301	0.0323	0.0252
Animal 2	0.0195	0.0225	0.0180
Animal 3	0.0202	0.0191	0.0327
Mean	0.02326 $\pm$ 0.0059	0.02463 $\pm$ 0.0073	0.02530 $\pm$ 0.0068

All regions of the uterus were found to have the three layers namely the endometrium, myometrium and the outer parametrium (Fig. 7).

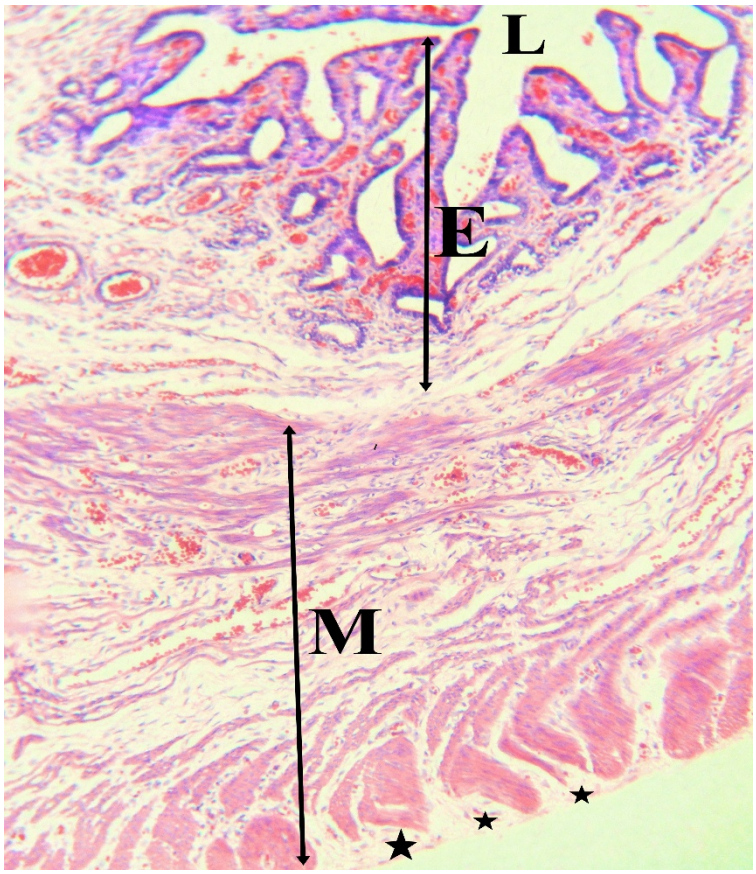

Figure 7: Structure of the uterus in gravid rabbits

A photomicrograph of the uterus of a Quintigravid rabbit showing the mural components, at X40 magnification, H and E staining. L is the lumen; E is the endometrium and the myometrium (M), the outermost layer is the parametrium depicted by the asterix.

3.1.1 ENDOMETRIAL GLAND DUCT DENSITY AND SIZE

The endometrium of the uteri studied comprises of an epithelial lining and the endometrial stroma. In all cases the epithelium was of the simple columnar type. Simple tubular glands lined by a columnar epithelium ran from the lining epithelium into the endometrial stroma. Found within the endometrial stroma were blood vessels and loose connective tissue.

In the mid-cornual endometrium, the mucosa of the primigravid endometrium (group 1) had a predominance of simple tubular endometrial glands. Simple columnar cells lined these glands. These cells contained hyperchromatic nuclei. In the second group (bigravid-quartigravida) and the group 3 rabbits (> quintigravid) had fewer endometrial glands compared to the primigravid. The cells lining these glands displayed columnar morphology, with hyperchromatic nuclei. With a rise in parity it was also noted that the glands have a wider lumen. The glandular epithelium in the quintigravid endometrium also exhibited papillary-like projection (Fig. 9C). The endometrium bordering the fallopian tube displayed similar characteristics as reported above. In the region of the cervix, the endometrium appeared similar in all the parity groups (Fig.10). The mucosa in all the groups in this region exhibited papillary-like projections into the lumen (Fig. 10).

Endometrial gland density of the uterine mucosa at the mid-cornual section was determined as described in the methodology section above. The proportion of the endometrial glands/ducts within the endometrial stroma was 45% in the primigravid group, 34% in the biparous-quadriparous rabbits and 37.5% in the multiparous rabbits. The results are as shown in the bar chart (Fig. 8) below. The luminal circumference of the endometrial glands/ducts was noted to increase with a rise in parity as shown in Table 5

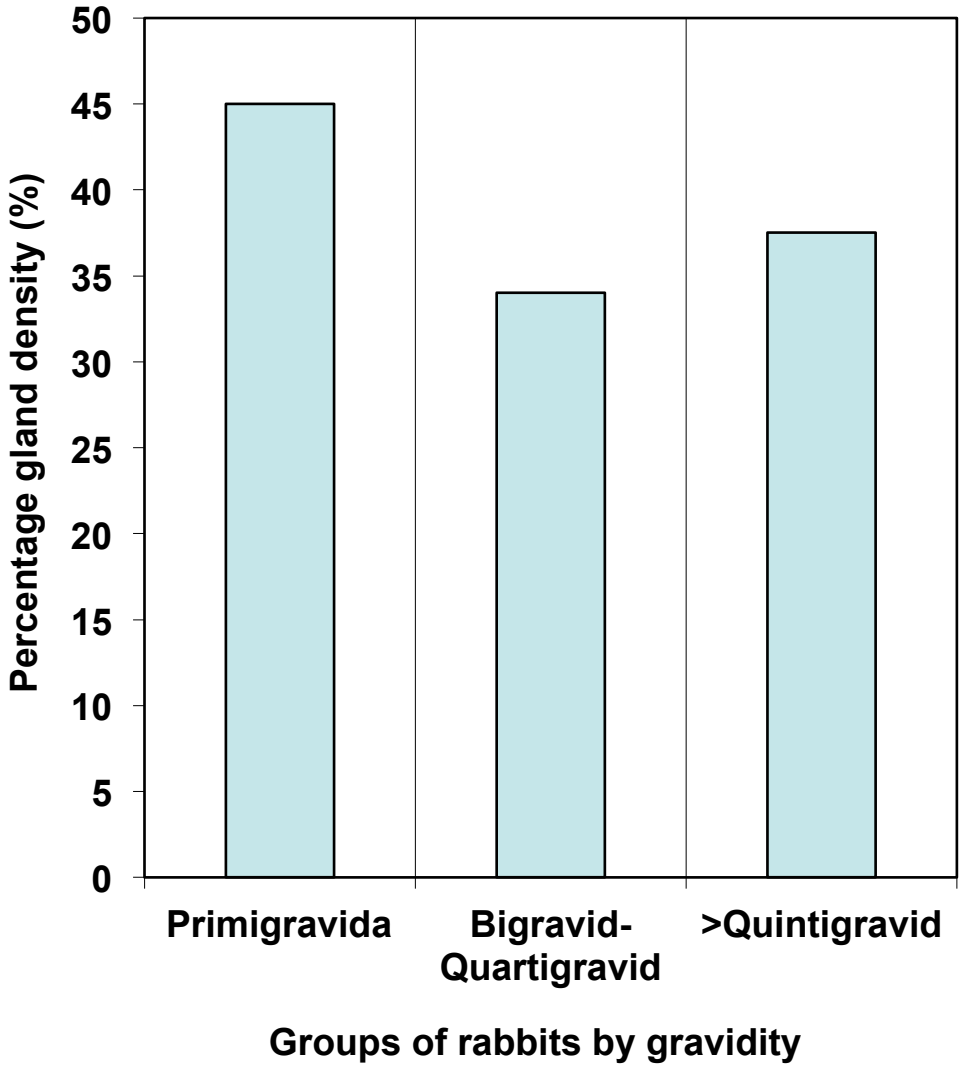

Figure 8: Chart of endometrial gland density in the different parity groups

Table 5: Illustration of the difference in luminal endometrial gland density in the different parity groups

Parity of the Rabbits	Luminal circumference of endometrial glands in micrometers (μm)
Primigravida	247.13 ± 0.02
Bigravida-Quartigravida	771.86 ± 0.01
> Quintigravida	797.31 ± 0.01

Circumferences of lumen of endometrial glands in the different parity groups, P=0.01. The values are given as mean ± SD

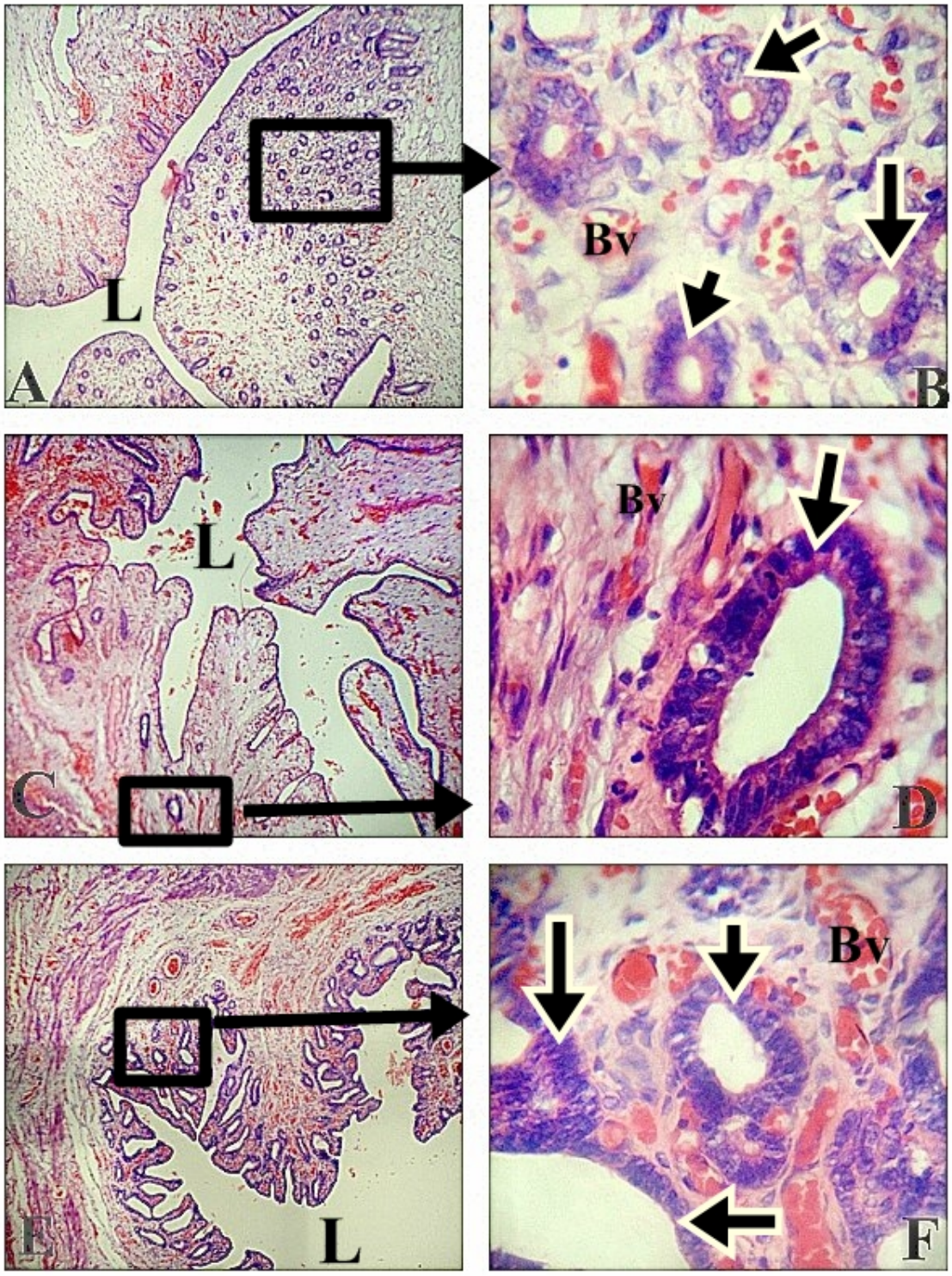

Figure 9: Distribution of endometrial glands in the different parity groups

Endometrial glands in the different parity groups stained with H and E:

A: The endometrium of a primigravid uterus taken at the mid-cornual section, at X100. Note the numerous endometrial glands (arrows).

B: B is inset from the rectangle in A at a higher magnification, X400, Note the hyperchromatic nuclei of the simple columnar cell lining the gland as shown by the arrow and the narrow glandular lumen. Bv is for blood vessels

C: The endometrium of bigravid uterus at the mid-cornual section, at X100. Note that the endometrial glands (arrows) are fewer compared to A above.

D: The endometrium of bigravid uterus at the mid-cornual section, at a higher magnification, X400, the lumen of the glands (shown by arrows) is larger. Bv is for the blood vessels with red blood cells within them.

E: The endometrium of quintigravid uterus at the mid-cornual section, at X100. Note that the endometrial glands are fewer compared to A above. Papillary-like projections of the mucosa project into the lumen L.

F: The endometrium of quintigravid uterus at the mid-cornual section, at a higher magnification, X400, reveals a wider glandular lumen and the hyperchromatic nuclei of the simple columnar cell lining the gland as shown by the arrow.

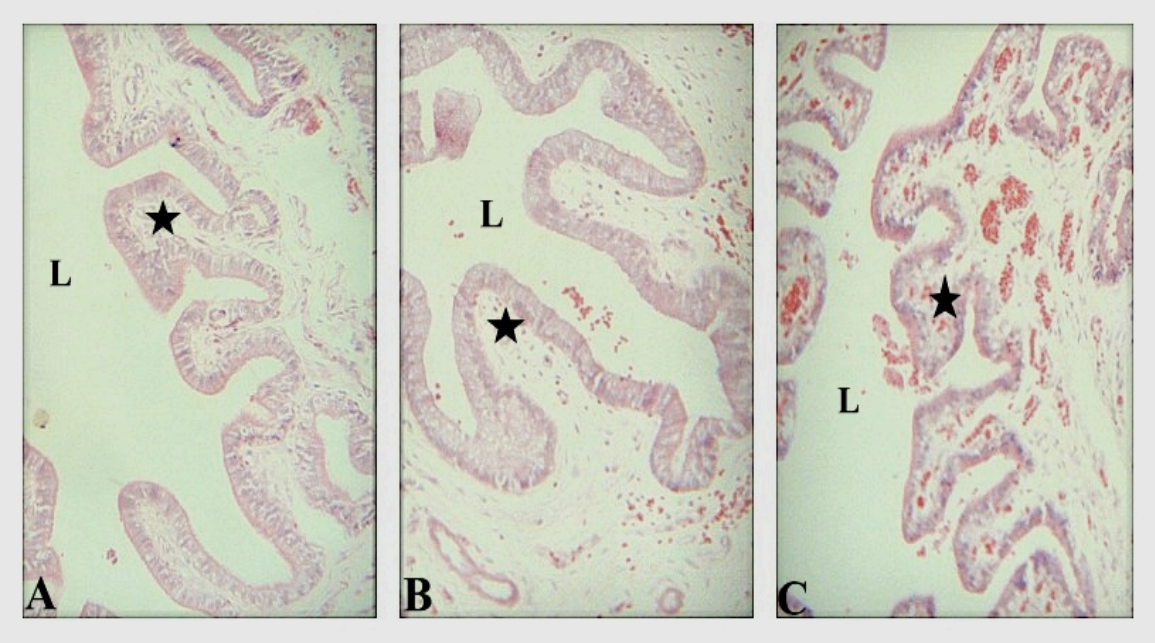

Figure 10: Illustration of the cervical mucosa

Similarity of the cervical mucosa in the different parity groups (H and E stain):

A: The mucosa of the cervical region in a primigravid rabbit at X100, L is the lumen. The asterix shows the papillary projections of the mucosa.

B: The mucosa of the cervical region in a tertigravid rabbit at X100, L is the lumen. The asterix shows the papillary projections of the mucosa.

C: The mucosa of the cervical region in a Quintigravid rabbit X100 magnification, L is the lumen. The asterix shows the papillary projections of the mucosa.

3.1.2 VASCULAR DENSITY OF THE ENDOMETRIAL STROMA AND THE MYOMETRIUM

The endometrial stroma was examined for vascularity. In all the groups an abundance of blood vessels was observed. However, the vessels increased as the parity increased such that the multiparous endometrial stroma displayed the most blood vessels (Fig.11).

The same feature was observed with the sections taken closer to the fallopian tube and at the cervix (Fig.12 and Fig.13 respectively). The vascular density of the endometrial stroma of the three regions of the uterus has been presented in **table 6**. The endometrial stroma of the multiparous female exhibited the highest vascular density in the three regions.

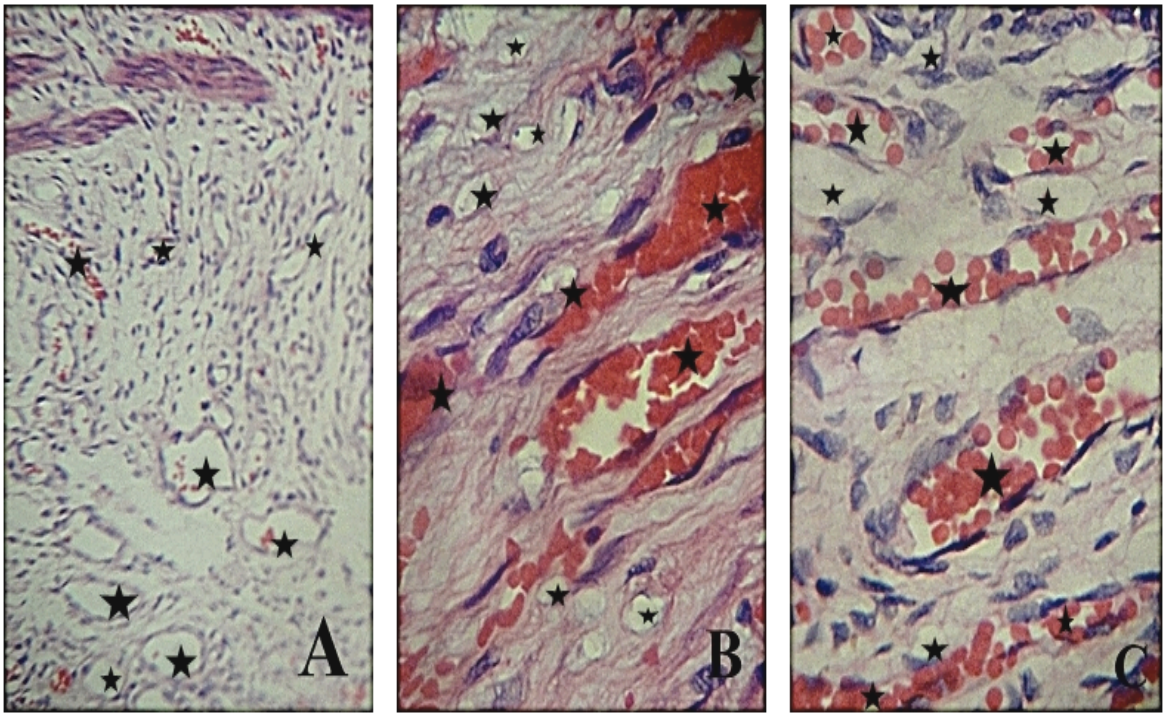

Figure 11: Blood supply of the mid-cornual region of the endometrial stroma

Stroma of the endometrium in the three parity groups at X 400 magnification, H and E stain, at the mid-cornu section of the uterus.

A: Stroma of the endometrium of a primigravid rabbit at the mid-cornu region. Blood vessels with red blood cells within them are shown by the stars.

B: Stroma of the endometrium of a tertigravid rabbit at the mid-cornu region. Blood vessels, within which are red blood cells are shown by the stars.

C: Stroma of the endometrium of a quintigravid rabbit at the mid-cornual region. Blood vessels are shown by the stars. Note that the blood vessels increase progressively, such that C has the most blood vessels.

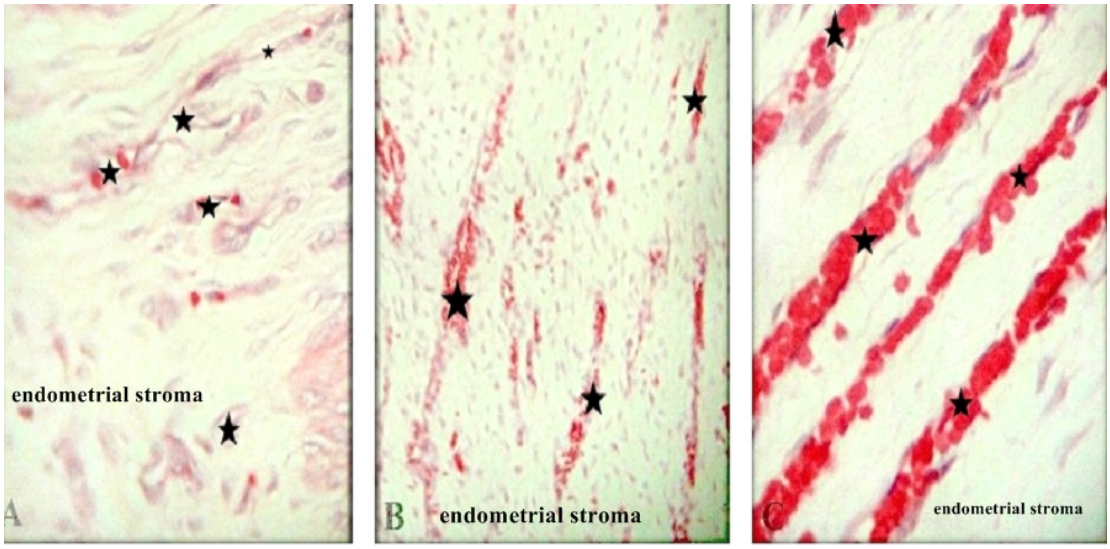

Figure 12: Blood supply of the endometrium in region bordering the fallopian tube

Stroma of the endometrium at part bordering the fallopian tube, at X100, H and E stain.

A: Stroma of the endometrium of a primigravid rabbit at the part bordering the fallopian tube. Note that blood vessels (asterix) are fewer in comparison to photomicrographs B and C.

B: Stroma of the endometrium of a tertigravid rabbit at the part bordering the fallopian tubes. The vessels (asterix) are fewer in comparison to photomicrograph C

C: Stroma of the endometrium of a quintigravid rabbit at the section bordering the fallopian tubes. The vessels (asterix) in this photomicrograph are more compared to A and B.

Table 6: Vascular density in the endometrial stroma in different parts of the uterus

Parity of the Rabbits	Vascular density in the endometrial stroma of the mid-cornual section (%)	Vascular density of the endometrial stroma of the part of the uterus bordering the tubes (%)	Vascular density of the lamina propria of the cervical mucosa (%)
Primigravida	15.8	11.1	16.3
Bigravid-Quartigravid	37.0	33.3	46.4
> Quintigravid	46.2	61.1	62.2
P value	0.02	0.01	0.01

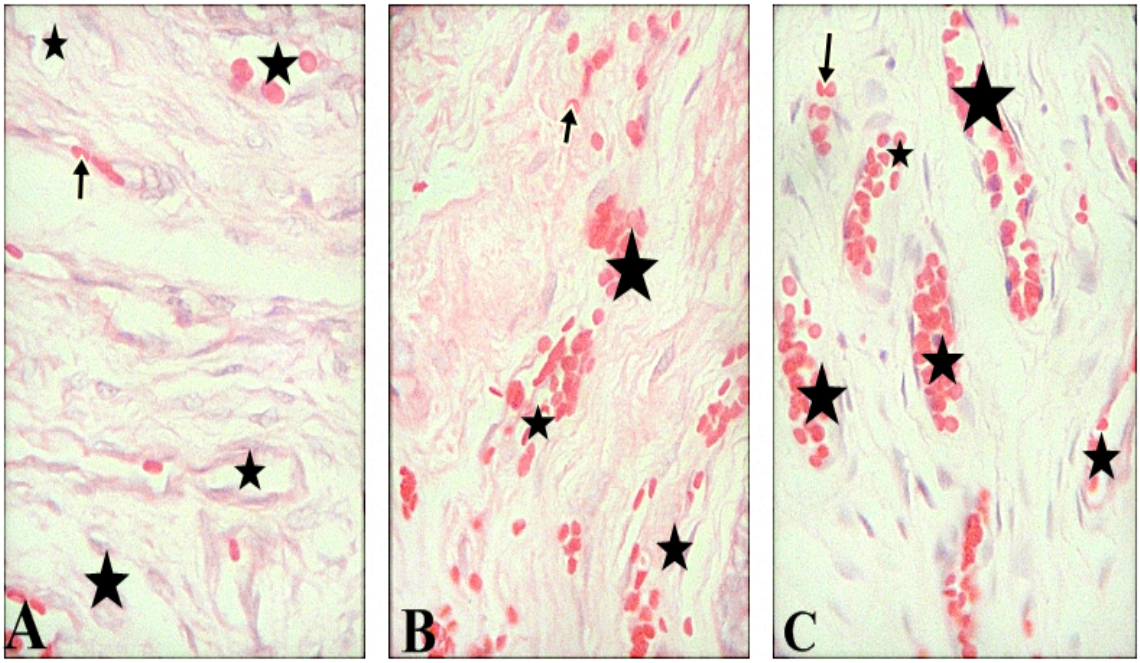

Figure 13: Blood supply of the cervical mucosa

Increase in vascular density with a rise in parity within the stroma of the cervical epithelium at X 100, after H and E staining.

A: Stroma of the cervical mucosa of a primigravid uterus. The blood vessels (asterix) are fewer in comparison to photomicrographs B and C. the arrows are pointing on the red blood cells within the vessels

B: Stroma of the cervical epithelium of a tertigravid uterus. The vessels are fewer in comparison to photomicrographs C.

C: Stroma of the cervical epithelium of a quintigravid uterus. The vessels in this picture are more compared to A and B.

As parity increased, the vascular density within the myometrium also increased, such that the primigravid myometrium was less vascular than the multiparous gravid myometrium (Fig. 14).

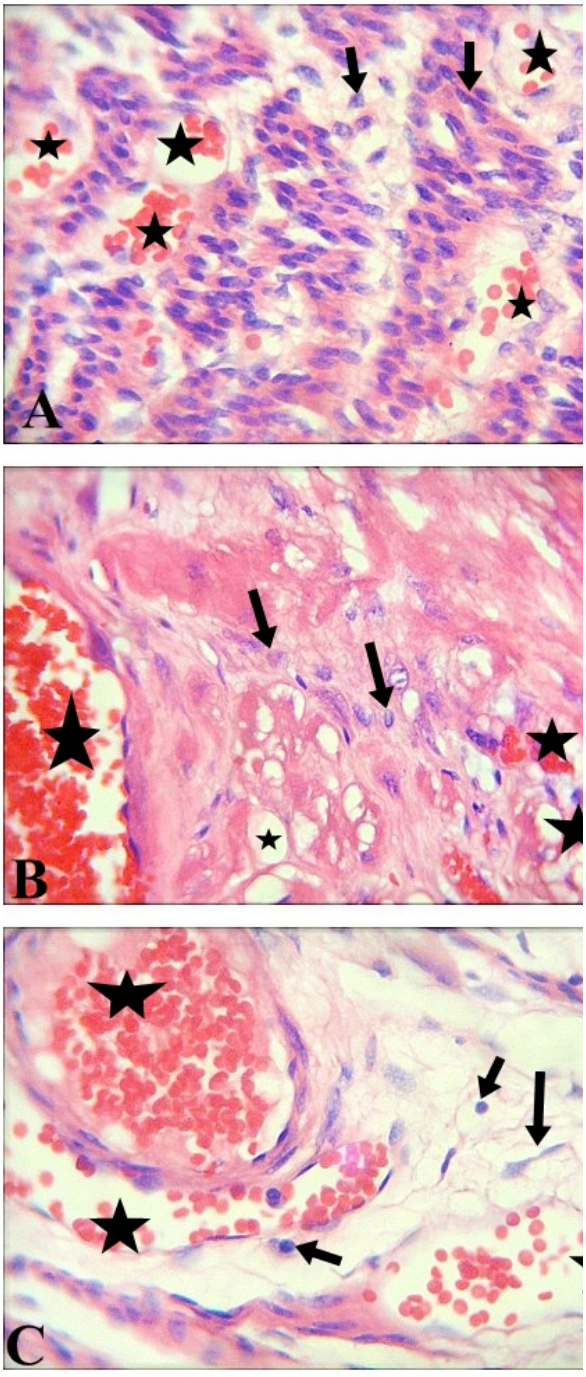

Figure 14: Illustration of myometrial vascularity in the different parity groups

Distribution of blood vessels in the "vascular zone" of the myometrium

A: Section taken from the mid-cornual primigravid uterus, focusing on the middle zone of the myometrium (vascular zone), H and E stain, at X400 magnification. Note the numerous smooth muscle cells (arrows pointing on their nuclei) and the smaller vessels (asterix),

B: Section taken from the mid-cornual section of a bigravid uterus, vascular zone of the myometrium, at X400, H and E stain. The smooth muscle cells are less compared to A above. The blood vessels, shown by asterix, are larger and numerous

C: Section of a quintigravid uterus, vascular zone of the myometrium, stained with H and E at X400 magnification. Note the larger blood vessels with red blood cells within (asterix) and the fewer smooth muscle cells (arrows).

Across the width of the myometrium, the intermediate zone of the uterus is noted to have the most blood vessels and is designated; the vascular zone. Comparison of the different parts of the uterus revealed no regional variations in vascularity (Fig. 15). The consistent finding is that the myometrium of the multiparous uterus is more vascular.

The calculated vascular density within the vascular layer of the myometrium revealed that the multiparous gravid myometrium had the highest density (70%) while the primigravid was the least vascular layer (25%). The intermediate group had 45% of the vascular layer of the myometrium occupied by blood vessels (Fig. 16). These measurements were obtained from the mid-cornual section of the uterus. The specimens of the uterus obtained from the part bordering the fallopian tubes and the cervical region, revealed similar findings, with no notable regional variation (Fig. 15).

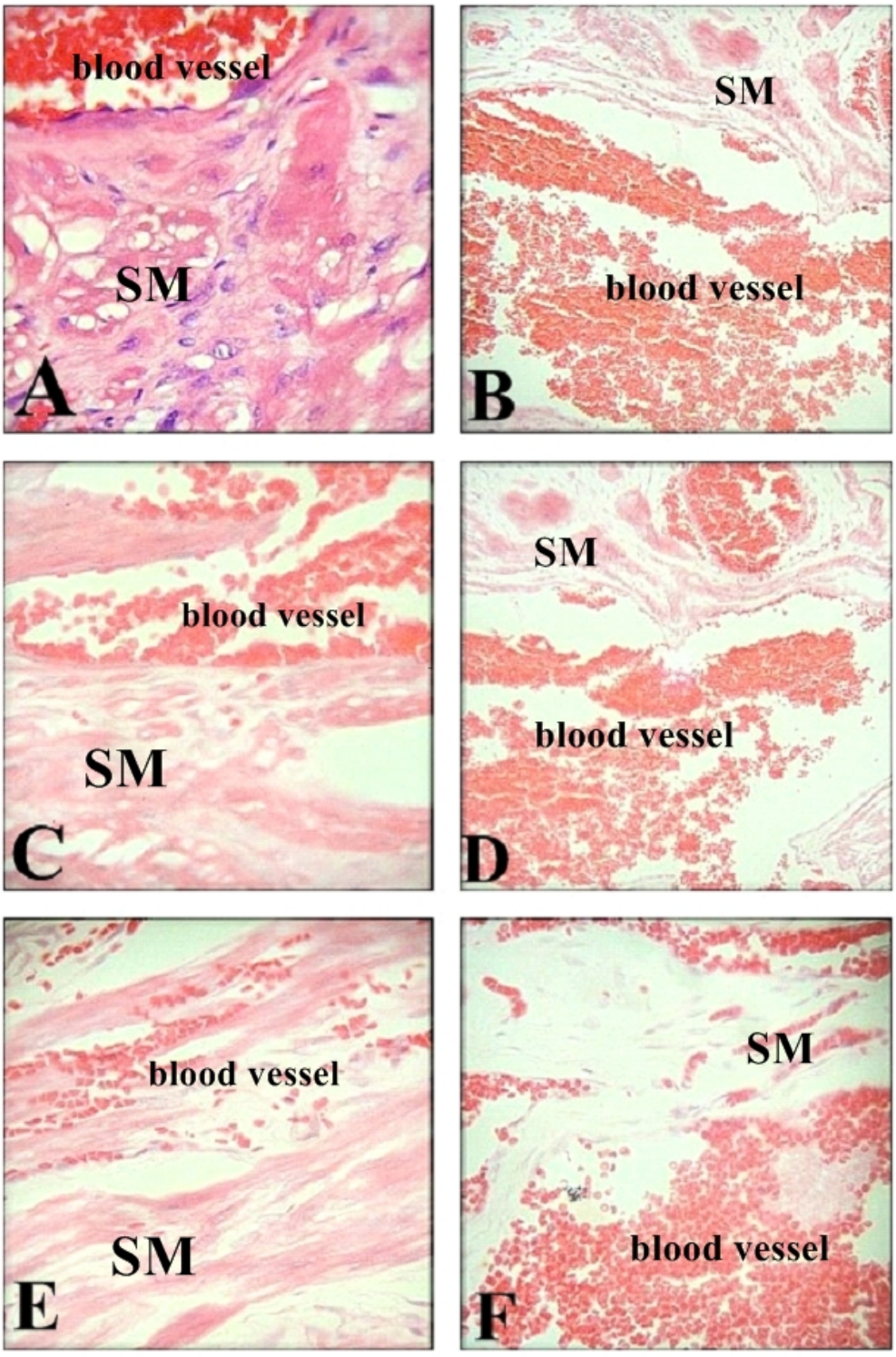

Figure 15: Blood vessels within the vascular zone of the myometrium

Distribution of blood vessels in the different parts of the myometrium, following H and E staining at X400. Photomicrographs A, C and E represent the group 2 rabbits (Bigravid-quartigravid), while B, D and F are the group 3 rabbits (>quintigravid). The first row is the myometrium at the mid-cornual region, the second at the part bordering the fallopian tubes and the last row at the cervical region.

Note that in all cases the multiparous myometrium (group 3) has more blood vessels than the intermediate group (group 2). Additionally, no regional differences in vascular density were observed. SM is smooth muscle.

A: The myometrium of the mid-cornual section of a bigravid rabbit. Note that the vascularity is similar as C and E

B: Myometrium of the mid-cornual region of a quintigravid rabbit. Note that the vascularity is similar as D and F.

C: Myometrium of the region bordering the fallopian tube of a bigravid rabbit.

D: Myometrium of the region bordering the fallopian tube of a quitigravid rabbit.

E: Myometrium of the cervical section of a bigravid rabbit.

F: Myometrium of the cervical section of a quintigravid rabbit.

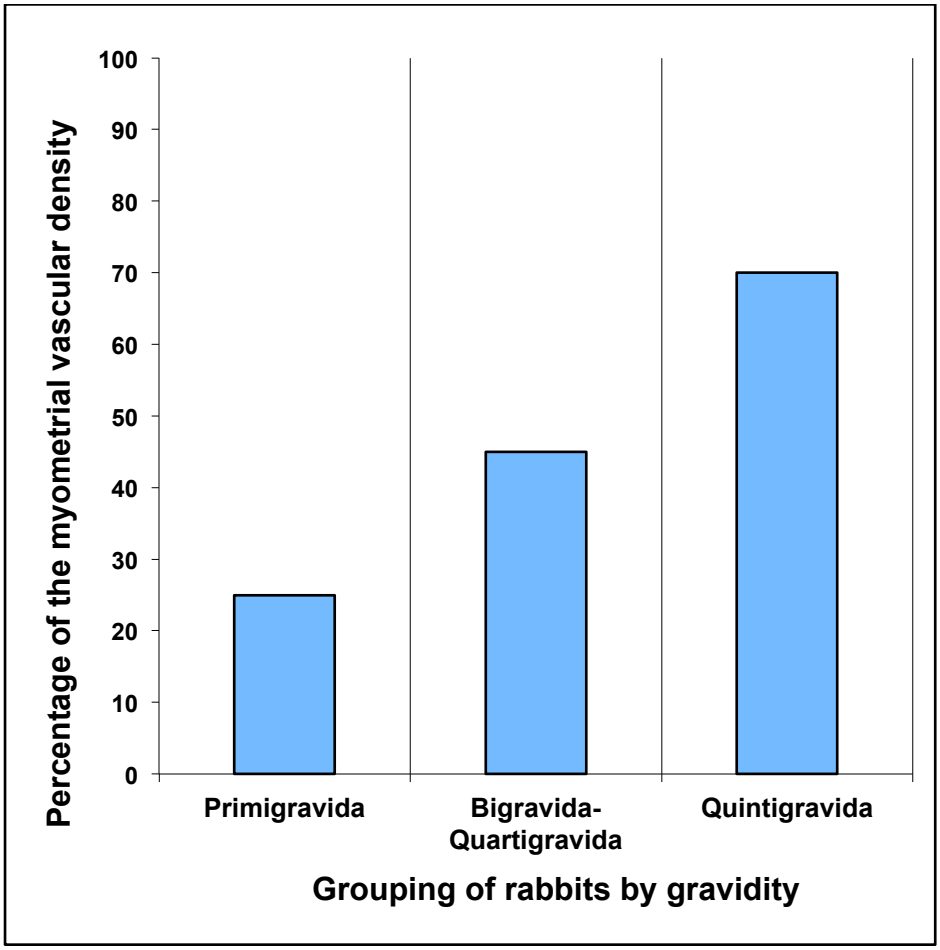

Figure 16: Regional variation in blood supply of the myometrium

3.1.3 MYOMETRIAL SMOOTH MUSCLE ORGANIZATION AND MYOMETRIAL THICKNESS

The myometrium of the primigravid uterus was noted to have the following characteristics irregular arrangement of the smooth muscle fibers. With a rise in parity, the muscular fibres were organized into inner circular and an outer longitudinal/oblique group. An even higher parity revealed an organization of the myometrium into three layers namely; the submucozal zone, the vascular layer and the supravascular layer (Fig. 17). The submucosal zone comprised tightly parked layer of circular smooth muscle fibers. The vascular layer consisted of fewer bundles of longitudinal muscles interspersed by blood vessels. The supravascular layer comprised tightly parked bundles of longitudinal muscles.

The primiparous rabbits were found to have 54.3% of the uterine wall occupied by the myometrium. The multiparous rabbits on the other hand had 70.6% of the uterine wall being the muscular layer. This figure was 67.4% in the intermediate group. The myometrial length was thickest in the multiparous rabbits. See Table 7. These findings were found to be statistically significant with a p value of 0.01.

Table 7: Myometrial thickness in the different parity groups

Parity of the Rabbits	Myometrial thickness (M) in mm (mean±SD)	Uterine wall thickness (U) in mm (mean±SD)	Myometrial thickness (M)/Uterine wall thickness (U) X100
1. Primigravid	0.44 ± 0.04	0.88 ± 0.06	50
2. Bigravid-Quartigravid	0.89 ± 0.04	1.32 ± 0.05	67.4
3. >Quintigravid	1.04 ± 0.01	1.47 ± 0.01	70.7

Figure 17: Disposition of myometrial smooth muscles

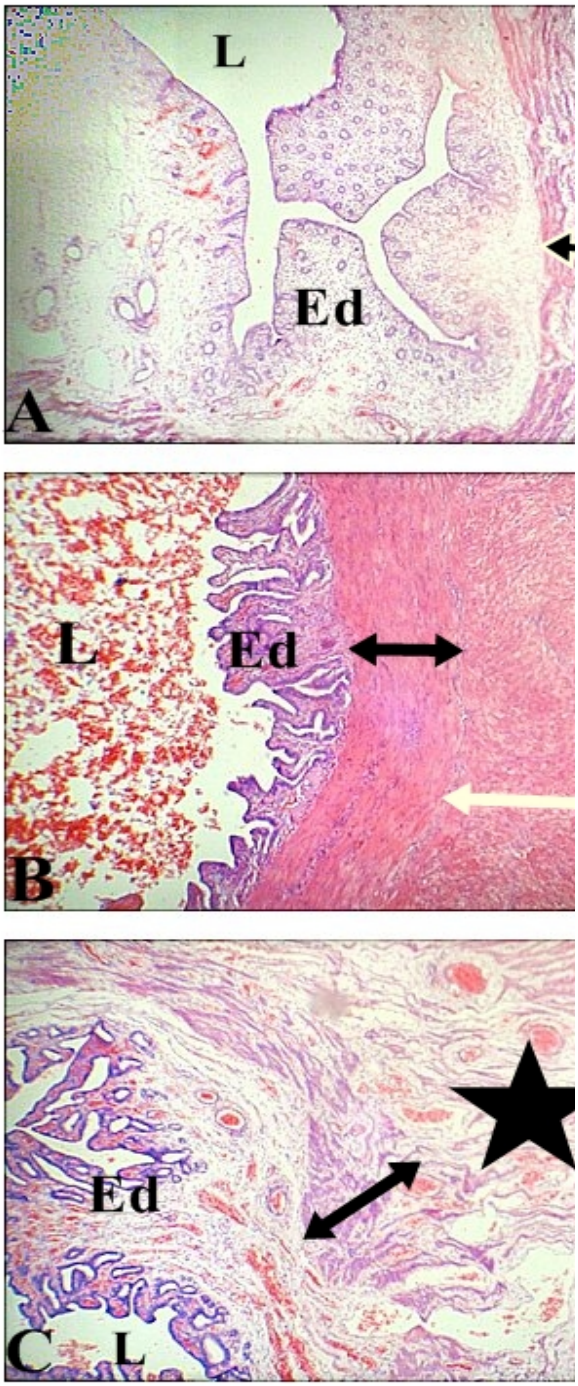

Organization of the myometrium in the different parity groups at X100, after H and E staining.

A: Myometrium of the mid-cornual section of a primigravid rabbit. Note that myometrium (arrow), has irregularly arranged smooth muscle fibres. L is the lumen, Ed is the endothelium.

B: Myometrium of the mid-cornual section of a bigravid rabbit. Note that in this picture, the myometrium is in two muscular layers; inner circular (black arrow) and outer longitudinal (white arrow). L is the lumen, Ed is the endothelium.

C: Myometrium of a quintigravid rabbit at the mid-cornual region. Of note is the organization of the myometrium into the three myometrial zones are more discernible; subendometrial (arrow), with circular smooth muscle, vascular (asterix), which is the largest, has blood vessels and interspersed longitudinal smooth muscle and the supravascular (arrow) comprising of longitudinally disposed fibers.

3.1.4 PROLIFERATION MARKER (Ki-67) AND ANTI-APOPTOTIC MARKER (BCL-2) IN THE ENDOMETRIUM AND MYOMETRIUM

In all the parity groups, more staining was noted in the glandular epithelium for the proliferation marker Ki-67 than the endometrial stroma (Fig. 18). The multiparous stroma stained more intensely for Ki-67 within the vascular elements as shown by the arrows (Fig.18D).

On the other hand, the anti-apoptotic marker Bcl-2 was noted to stain intensely on the luminal epithelium in all the parity groups (Fig.19). Of note, is the intense staining of the vascular tissue within the stroma of the quintigravid uterus as shown by the asterix (Fig.19D).

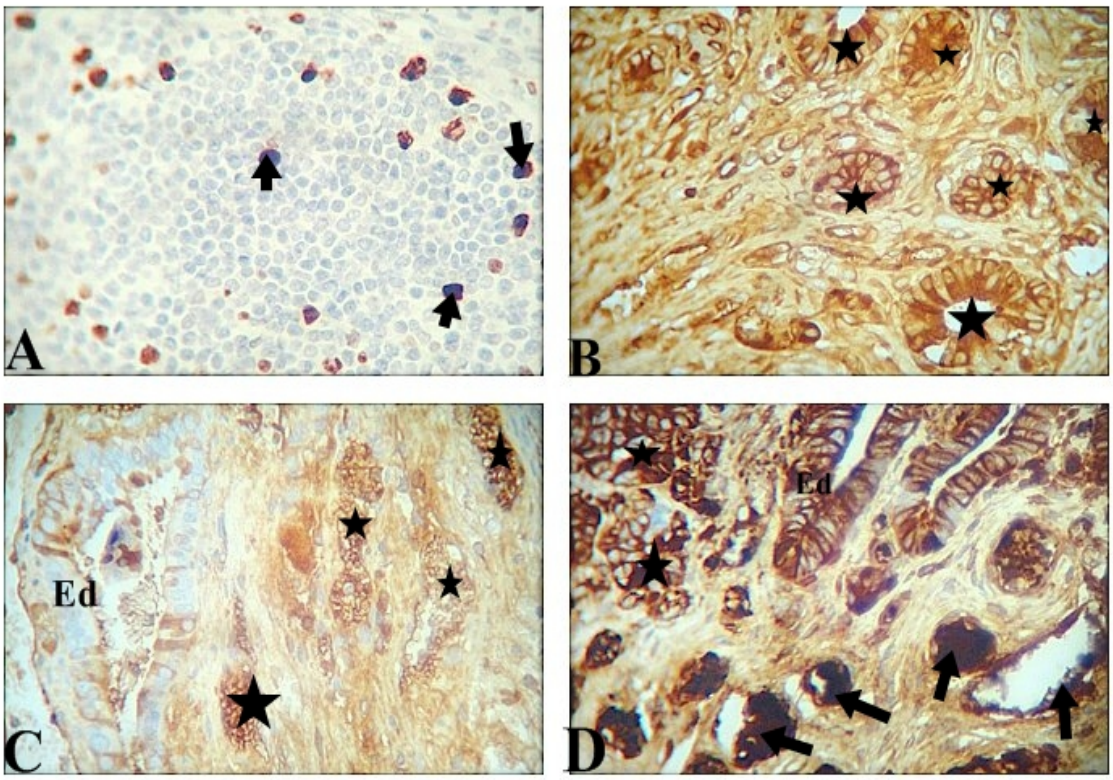

Figure 18: Distribution of the proliferation marker Ki-67 in the endometrium

Proliferation marker Ki67 on the endometrial glands in the different parity groups, at x400

A: Photomicrograph of the control, tonsillar tissue, after immunohistochemical staining at X400. The brown staining (arrows), is a positive finding, showing presence of the Ki-67 antigen within these cells.

B: Primigravid endometrium from the mid-cornual section at X400, after immunohistochemical staining. Note that the cells lining the glands stain positively for Ki-67 marker as shown by the asterix.

C: Bigravid endometrium from the mid-cornual region of the uterus at X400 following immunochemical staining. The cells of the glandular epithelium are staining brown as shown by the asterix. Notably, the glands in B above stain more strongly.

D: Photomicrograph of a quintigravid endometrium from the mid-cornual section of the uterus at X400. Note the more staining in the glandular epithelium than the lining epithelium. Ed is the lining epithelium, the asterix demonstrate the staining on the glandular elements. Also note the intense staining in D for the vascular tissue as shown by the arrows.

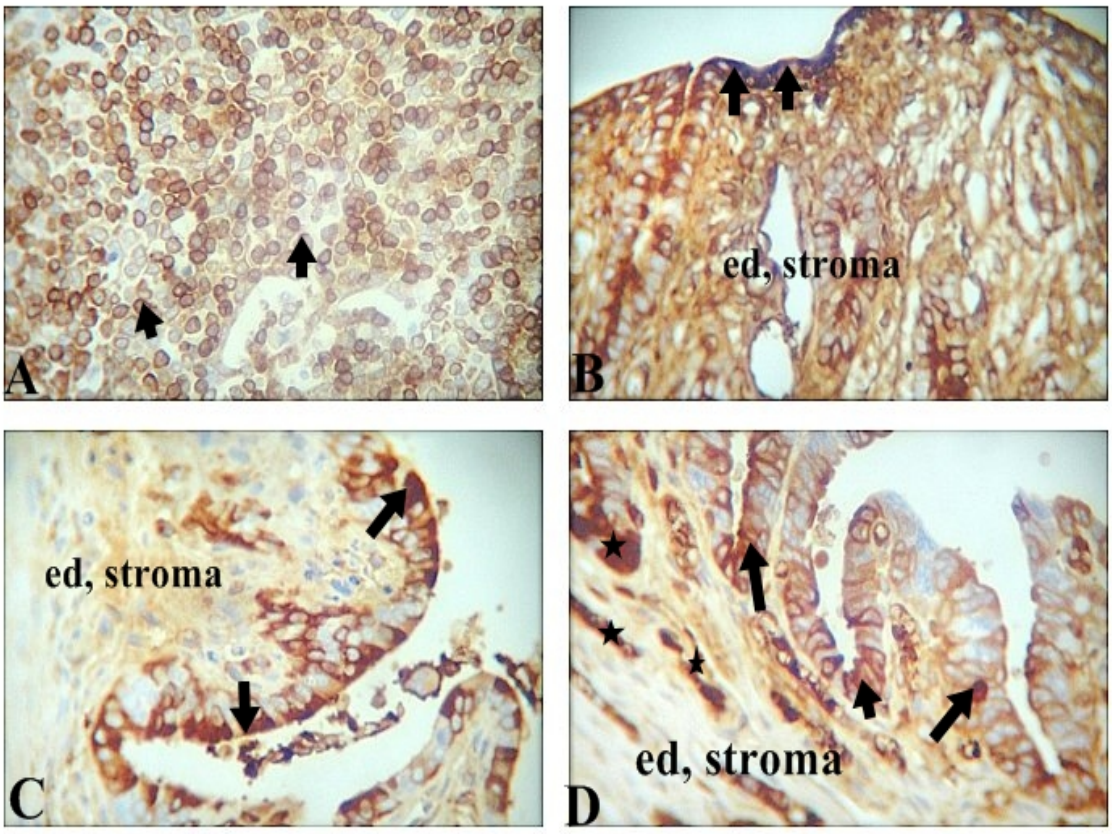

Figure 19: Distribution of the anti-apoptotic marker Bcl-2 in the endometrium

Bcl-2 on the endometrial stroma in the different parity groups, at magnification X400

A: Normal tonsillar tissue acting as a control following immunohistochemical staining at X400, the brown staining (arrows) denotes a positive finding within the cells of this tissue for the anti-apoptotic marker Bcl-2

B: Primigravid endometrium, mid-cornual section after immunohistochemical staining at X400. Note that the luminal epithelium (arrows) stains more strongly in comparison to the endometrial stroma (as shown by the arrows).

C: Bigravid endometrium at the mid-cornual section following immunohistochemical staining at x400. Note that the luminal epithelium stains brown while the endometrial stroma stains negatively in this section.

D:A quintigravid endometrium at the mid-cornual section following immunohistochemical staining at X400. Note that the luminal epithelium stains more strongly compared to the endometrial stroma as shown by the arrows. In addition the vascular channels in the multiparous endometrial stroma (D) stain with Bcl-2.

At the mid-cornual section, the primigravid and quintigravid myometrium were found to react positively with the marker for proliferation Ki-67 (Fig. 20). The intermediate parity group did not stain with this marker. The section bordering the fallopian tube demonstrated more staining in the

primigravid female, although fewer compared to the mid-cornual section, fewer in the quintigravid female and none in the intermediate group (Fig. 21). The cervical myometrium did not stain for Ki-67 (Fig. 22).

The staining for the anti-apoptotic marker Bcl-2 exhibited regional variation such that the section taken at the middle of the cornua, the primigravid uterus stained the most strongly with Bcl-2, followed by the quintigravid one. In the primigravid rabbits, it is the myometrial smooth muscle cells that stained whereas in the multiparous rabbits it is the vascular endothelial cells and the stromal cells. The bigravid rabbit did not stain for this marker (Fig. 23). In the uterus bordering the fallopian tube the primigravid myometrium stained positively. In this case, in both cases, it is the endothelial cells of the vascular channels that stained with Bcl-2. The bigravid and the quintigravid myometrium did not stain (Fig. 24). In the cervical section, the multigravid myometrium stained positively while the bigravid and the primigravid rabbits both stained negatively (Fig. 25).

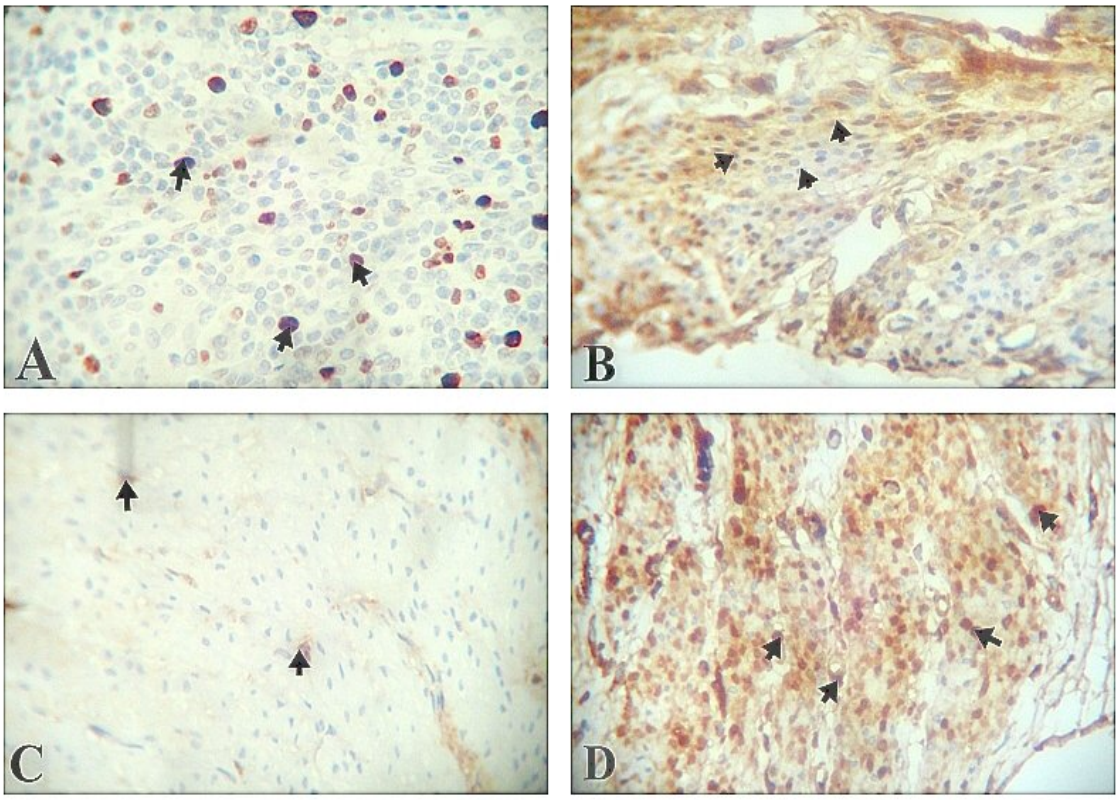

Figure 20: Variation of the proliferative marker Ki-67 in the mid-cornual part of the myometrium

A: A control, normal tonsillar tissue, following immunohistochemical staining for the proliferation marker Ki-67 at X400. The brown (arrows) staining indicates presence of this marker in these cells.

B: Mid-cornual section of the primigravid myometrium following immunohistochemical staining for the proliferation marker Ki-67 at X400. Note the presence of this marker in some cells of the uterus.

C: Myometrium taken from the mid-cornual region of a bigravid uterus following immunohistochemical staining for the proliferation marker Ki-67 at X400. Note that this section hardly has any brown staining.

D:Quintigravid myometrium from the mid-cornual region following immunohistochemical staining for the proliferation marker Ki67 at X400. Note the intense in this section. The cells containing this marker stain brown.

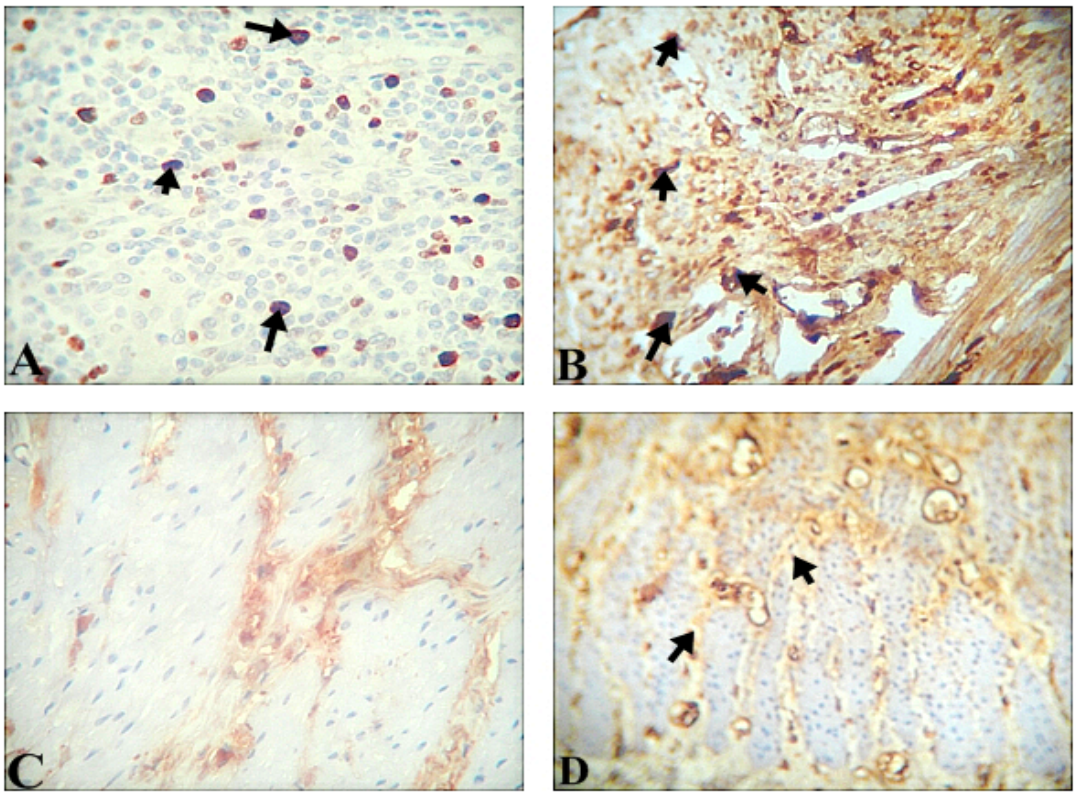

Figure 21: Proliferation marker Ki-67 in the part of the myometrium bordering the fallopian tubes

Staining for the proliferation Ki-67 in the part of the myometrium bordering the fallopian tubes

A: Normal tonsillar tissue following immunohistochemical staining for the proliferation marker Ki-67 at X400. The brown (arrows) staining indicates presence of this marker in these cells.

B: Primigravid myometrium in the part adjacent to the fallopian tubes following immunohistochemical staining for the proliferation marker Ki-67 at X400. Note the presence of this marker in the cells of the myometrium, more so along the lining of blood vessels.

C: Myometrium taken from the region of the uterus closest to the fallopian tubes of a bigravid uterus following immunohistochemical staining for the proliferation marker Ki-67 at X400. Note that this section hardly has any brown staining. However, the vascular channels stain positively.

D: Quintigravid myometrium from the part bordering the fallopian tubes, following immunohistochemical staining for the proliferation marker Ki-67 at X400. Note that it is the lining of blood vessels that stain positively for this marker.

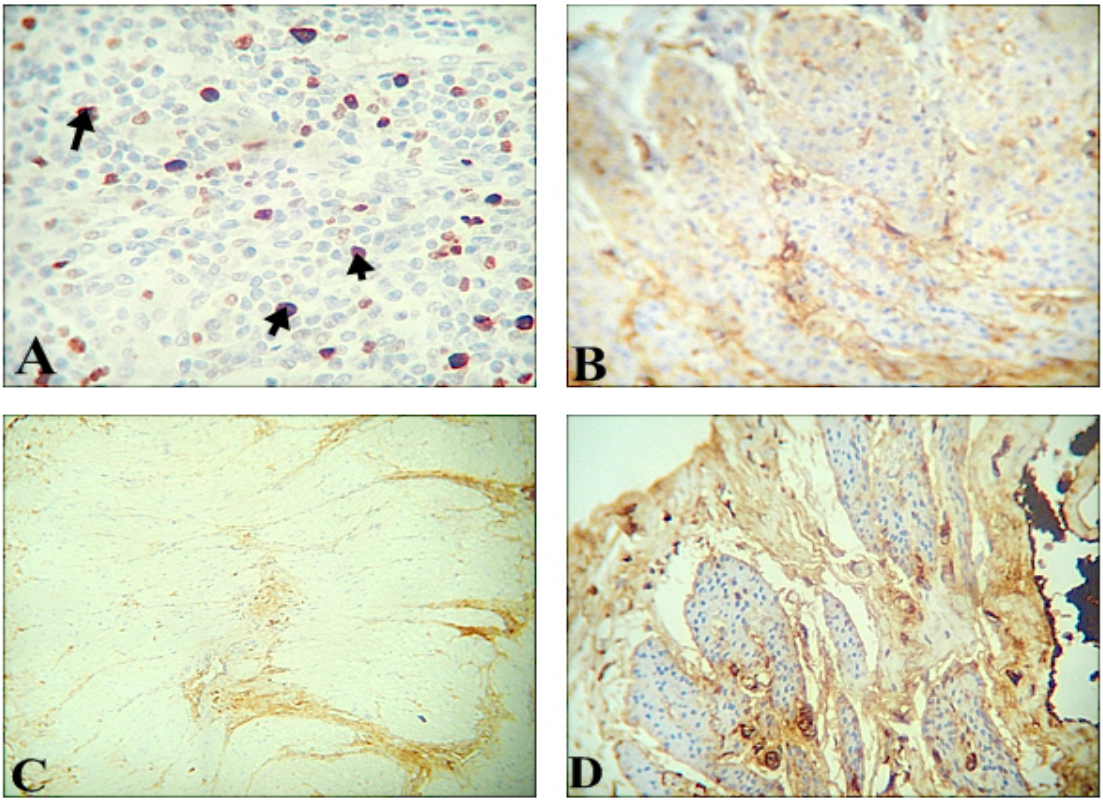

Figure 22: Distribution of the proliferation marker ki-67 in the fibromuscular part of the cervix

Staining for the proliferation Ki-67 in the part of the cervical region of the uterus in the different parity groups

A: Normal tonsillar tissue following immunohistochemical staining for the proliferation marker Ki-67 at X400. The brown (arrows) staining indicates presence of this marker in these cells.

B: Primigravid fibromuscular layer of the cervix, following immunohistochemical staining for the proliferation marker Ki-67 at X400. Note the absence of this marker in the section. The brown staining is noted along the vascular lining.

C: Bigravid fibromuscular layer of the cervix, following immunohistochemical staining for the proliferation marker Ki-67 at X400. Note that this section hardly has any brown staining. However, the vascular channels stain positively.

D: Quintigravid fibromuscular layer of the cervix, following immunohistochemical staining for the proliferation marker Ki-67 at X400. Note that it is the lining of blood vessels that stain positively for this marker.

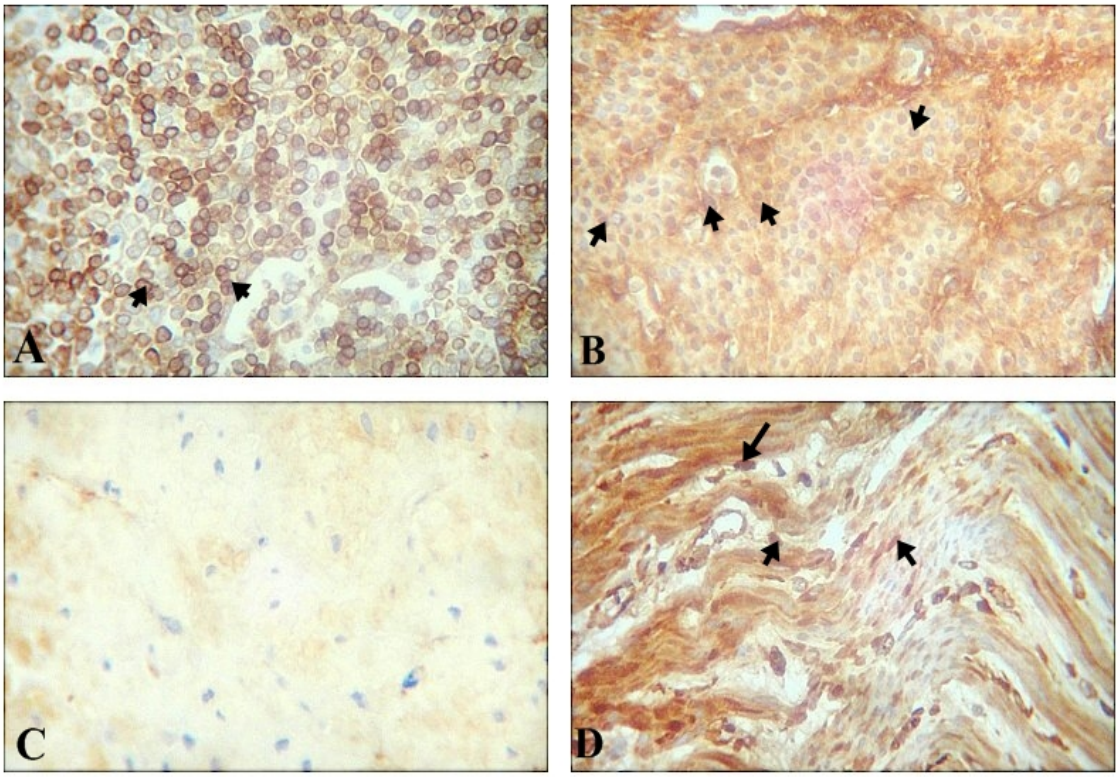

Figure 23: Variation of the Bcl-2 protein in the mid-cornual part of the myometrium

Staining for the anti-apoptotic marker Bcl-2 in the myometrium, mid-cornual section

A: Normal tonsillar tissue, following immunohistochemical staining for the proliferation marker Bcl-2, at X400. Cells containing this anti-apoptotic marker take the brown stain (arrows).

B: Primigravid myometrium, staining for anti-apoptosis marker Bcl-2 at the mid-cornual section at x400. Note the numerous brown stained cells (arrows).

C: Bigravid myometrium, mid-cornual section staining for anti-apoptosis marker Bcl-2 at the mid-cornual section at x400. Note that the cells in this section are devoid of the brown stain.

D: Multigravid myometrium staining for anti-apoptosis marker Bcl-2 at the mid-cornual section at x400. Note that some cells in this section take up the brown stain. Also note the presence of the brown stain in the lining of the blood vessels.

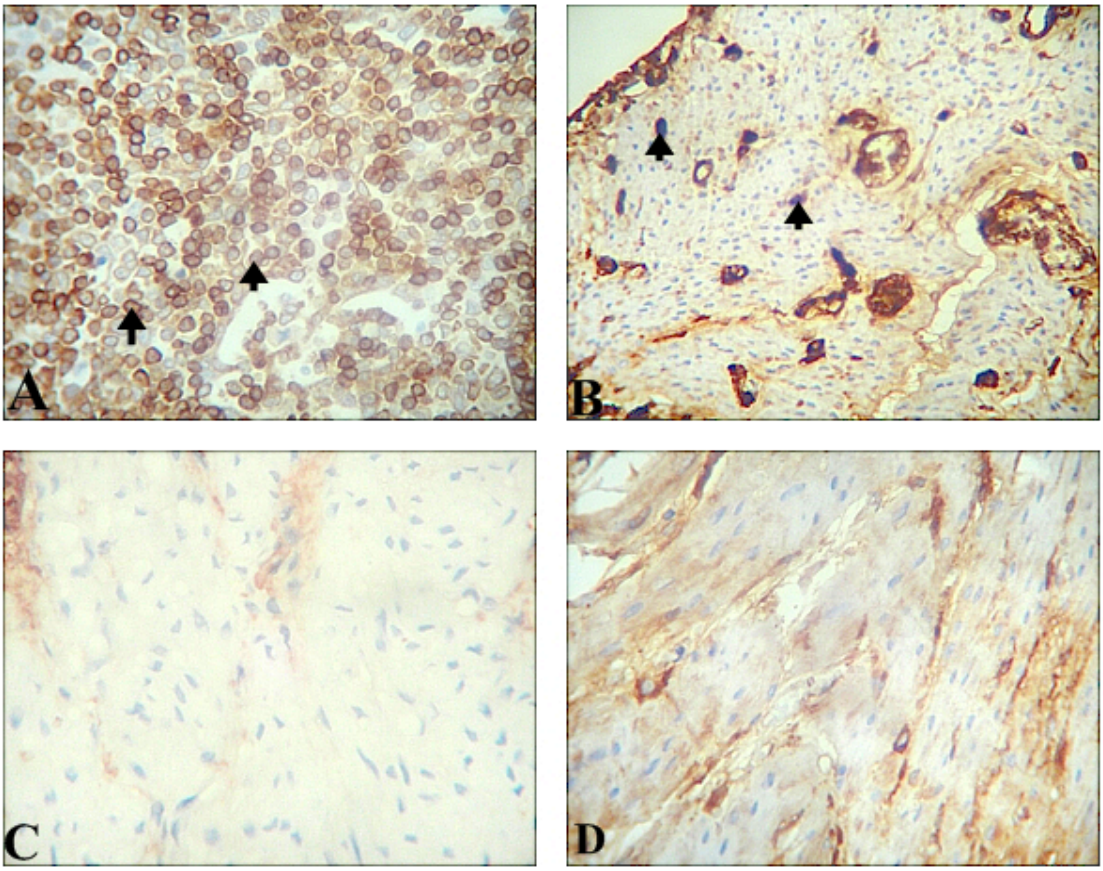

Figure 24: Distribution of Bcl-2 protein in the part of the myometrium bordering the fallopian tubes

Staining for the anti-apoptotic marker Bcl-2 in the myometrium, part bordering the fallopian tubes

A: Normal tonsillar tissue, following staining for the proliferation marker Bcl-2, at X400. Cells containing this anti-apoptotic marker take the brown stain (arrows).

B: Primigravid myometrium, staining for anti-apoptosis marker Bcl-2 at the part adjacent to the fallopian tubes at x400. Note the numerous brown stained cells (arrows) as well as the intense staining in the blood vessels.

C: Bigravid myometrium, part adjacent to the fallopian tube staining for anti-apoptosis marker Bcl-2 at the mid-cornual section at x400. Note that the cells in this section are devoid of the brown stain. However the vascular channels stain brown

D: Quintigravid myometrium staining for anti-apoptosis marker Bcl-2 at the part adjacent to the fallopian tubes at x400. Note that some cells in this section take up the brown stain. Also note the presence of the brown stain in the lining of the blood vessels.

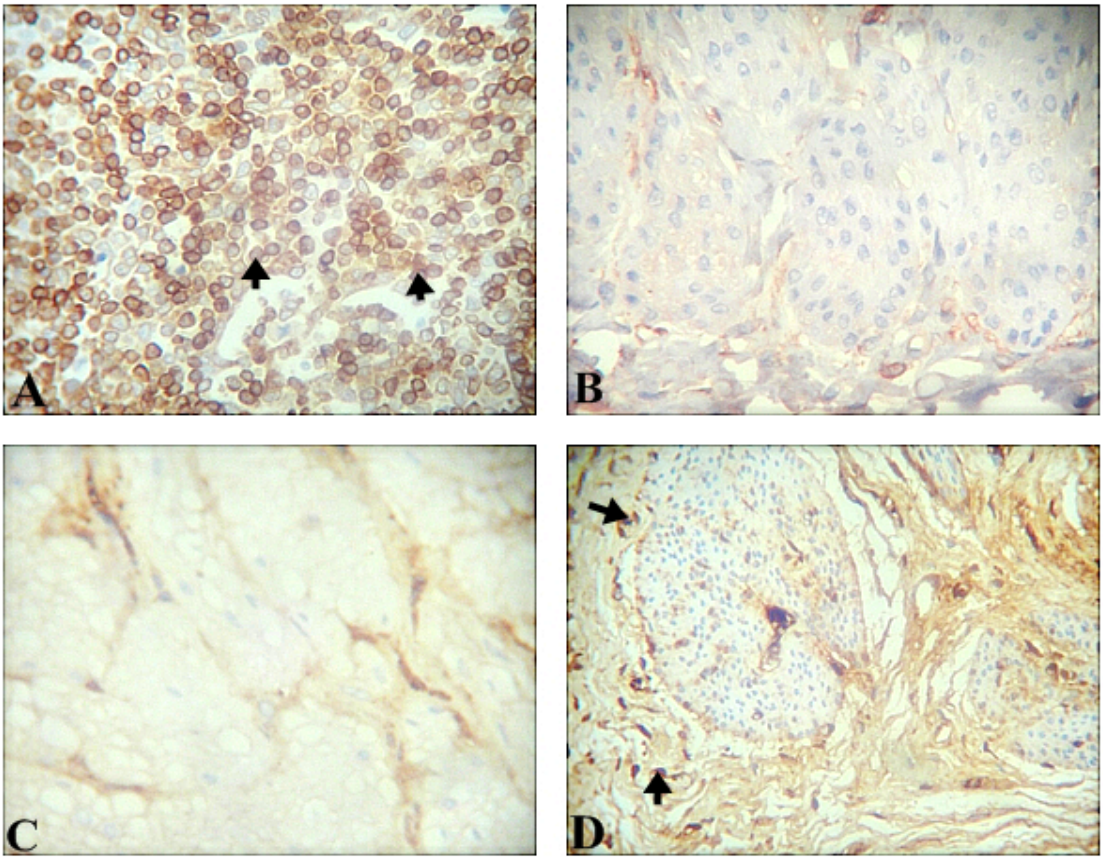

Figure 25: Distribution of the Bcl-2 protein in the fibromuscular part of the cervix

Variation in staining for the anti-apoptotic marker Bcl-2 in cervical fibro-muscular region.

A: Normal tonsillar tissue, following immunohistochemical staining for the proliferation marker Bcl-2, at X400. Cells containing this anti-apoptotic marker take the brown stain (arrows).

B: Primigravid cervical fibro-muscular region, staining for anti-apoptosis marker Bcl-2 at x400. Note the cells in this section have not taken the brown stain. However, the cells lining the vascular channels have.

C: Bigravid cervical fibro-muscular region staining for anti-apoptosis marker Bcl-2 at the mid-cornual section at x400. Note that the cells in this section are devoid of the brown stain. However the vascular channels stain brown

D: Quintigravid myometrium staining for anti-apoptosis marker Bcl-2 at cervical fibro-muscular region at x400. Note that very few cells in this section take up the brown stain. Also note the presence of the brown stain in the lining of the blood vessels.

CHAPTER FOUR: DISCUSSION

4.1 GENERAL FINDINGS

Observations of the present study reveal a rise in body mass-normalized uterine weight as the parity ascends. These findings were however not statistically significant. Other uterine parameters that have been shown to correlate positively with parity include uterine volume and uterine diameters (Olayemi et al., 2002). These differing uterine parameters due to parity may be as a result of retained changes of uterine remodeling that have occurred in previous pregnancies. Indeed, uterine involution has been shown to be affected negatively by parity such that it is much slower in multiparous females (Negishi et al., 1999, Zduńczyk et al., 2004, Zhang et al., 2010). On the contrary, Ababneh and Degafa, (2005) established that uterine involution is not affected by parity suggesting that there may be other explanations to these findings.

The typical layers of the uterus were observed in the pregnant rabbits used in this study the endometrium, myometrium and parametrium. Known differences between a gravid and non-gravid uterus include; thicker luminal and glandular epithelium, numerous highly coiled stromal glands as well as a thicker myometrium (Cruz and Selwood, 1997). Progesterone is the key hormone of pregnancy that prepares the uterus for implantation and maintenance of the conceptus and is therefore responsible for these pregnancy related changes (Nasar and Rahman, 2006, Young, 2010,).

In all the rabbits, the glandular and lining epithelia were of the simple columnar type with hyperchromatic nuclei. It is known that the endometrium retains a columnar morphology in pregnancy (Roberts et al., 1984). Studying rats, Intan-Shameha et al., (2005), established that the cells of the uterine mucosa become taller in pregnancy and occasionally stratification is observed. A loss of the columnar morphology may not be unusual as it has been reported in monkeys (Rosario et al., 2007). Multinucleation of the endometrial lining as a result of fusion of the columnar cells can also occur in pregnancy (Davies and Hoffman, 1973). These changes that occur on the endometrial epithelium in pregnancy are referred to as the Arias-Stella reaction and were first described by Javier Arias-Stella (Arias-Stella, 1954). They comprise nuclear enlargement, hyperchromatism with cytoplasmic swelling and vacuoles. The main characteristic of the reaction is cellular enlargement, mainly of the nucleus to double or many times its usual size.

4.2 ENDOMETRIAL GLAND DUCT DENSITY AND SIZE

In the present study, there was a decrease of gland duct density within the endometrium with a rise in parity in pregnant rabbits, such that the percentage proportion within the endometrial stroma was 45%, 34% and 37.5% in the primiparous group, biparous-quadriparous and multiparous groups respectively. To the best of our knowledge, this is the first study correlating endometrial glands with

parity. The findings of this study could provide some explanation of observations of previous studies. For example, endometrosis also known as chronic degenerative endometrial disease is characterized by reduced endometrial glands. This condition has been shown to correlate positively with a rise in parity in mares as opposed to age (Bracher et al., 1996). It is therefore possible that the progressive loss if endometrial glands in higher parity groups as observed in this study is part of a physiological degeneration.

It is known that endometrial carcinoma is more common in nulliparous and low parity females (Albrektesen, 2009). Reduction in endometrial glands as the parity rises may be the reason why parity is protective against endometrial cancer. Repeated strong exposure to progesterone has been thought to play a protective role. While studying the effect of progesterone on non-pregnant bovine endometria, Wang et al., (2007), proposed that the increased endometrial gland density after estrogen exposure may be driven by changes in total endometrial area rather than by proliferation and regression of glandular cells. According to these authors, a smaller endometrial area gives an impression of higher glandular density.

In thoroughbred mares, surface endometrial gland density has been found to correlate positively with the greater surface density of placental cotyledons observed in these animals (Lefranc and Allen, 2007). In a separate study, multiparous mares were noted to have the lowest microcotyledons surface density (Wilsher and Allen, 2003). The lower density of placental cotyledons observed in multiparous females by these authors may be explained by the reduced endometrial gland density in the higher parity group as seen in the current study.

During pregnancy endometrial glands undergo extensive hypertrophy and hyperplasia to provide increasing histotrophic support for the conceptus (Finn and Martin 1976). The secretory products of endometrial glands are essential for the establishment of uterine receptivity and conceptus implantation (Gray et al., 2001a, b). Inhibition of postnatal growth of these glands via gene knock out resulted in infertility (Spencer and Gray 2006). Ewes that lack uterine glands and histotroph fail to exhibit normal estrous cycle or maintain pregnancy beyond day 14. Development of uterine glands (adenogenesis) in mammals typically begins in the postnatal period and involves budding of nascent luminal epithelium and extensive proliferation as they grow into the surrounding stroma, elongate and mature (Cooke et al., 2012). In rabbit, sheep and pig a servomechanism is proposed to regulate endometrial gland development and differentiated function during pregnancy. It involves sequential actions of ovarian steroid hormones, pregnancy recognition signals and lactogenic hormones from the pituitary and placenta (Gray et al., 2001). In the postpartum period, the endometrial glands undergo involution (Gray et al., 2003). A complete decline of progesterone shortly before parturition is what is responsible for the postpartum endometrial degeneration (Degafa et al., 2006). In the equine

endometrium rapid degeneration of the uterine glands occurs after pregnancy such that by day 7 postpartum the endometrial histology is similar to that observed during normal proestrous (Gray et al., 2001a, b). It is therefore plausible that the intensity of endometrial gland proliferation reduces as parity increases.

The current study observed that endometrial gland duct size increases with a rise in parity. While studying non pregnant bovine uteri, Wang et al., (2007), established that whereas high progesterone levels was associated with an increase in endometrial gland density, it was accompanied by a decrease in endometrial gland size. These findings are in agreement with what was observed in the pregnant rabbits used in this study. The primiparous rabbits had the highest endometrial gland density as well as the smallest gland duct circumference of 217 $\pm$ 0.02 μm compared to a duct circumference of 797 $\pm$ 0.01 μm in the multiparous females.

4.3 VASCULAR DENSITY OF THE ENDOMETRIAL STROMA AND THE MYOMETRIUM

The current study presents an increase in vascular density of the uterine mucosa as the parity rises. A study on non pregnant human females using a power Doppler, Ng et al., (2006), reported that parity is not one of the factors that affect uterine blood flow. According to these authors, parity, women's age and smoking habits did not affect endometrial blood flow while serum high estradiol concentrations reduced blood flow to the endometrium (Ng et al., 2006). It is possible that the findings of the current study are as a result of cumulative effect of endometrial remodeling in pregnancy. In sheep, endometrial angiogenesis during pregnancy has been shown to occur from pre-existing capillary networks (Grazul-Bilska et al., 2010).

In rabbits, during the early stages of pregnancy, as the cells of the uterine mucosa proliferates, there is an intense angiogenesis accompanied by a corresponding increase in vascular density (Parry, 1950). Given the early and prominent role that the endometrial vasculature plays in the endometrial response to the implanting blastocyst, it is thought that the vascular changes may contribute to uterine receptivity and subsequent fetal survival (Rogers, 1996). Indeed, weight and crown-rump length of the fetus have been shown to be significantly influenced by the number of the blood vessels reaching the endometrium such that the fewer the vessels the lower the weight (Argente et al., 2006). Interestingly, there is evidence that low parity is a risk factor for low birthweight (Mavalankar et al., 1992). It is therefore possible that the lower vascularity seen in endometrium of the primigravidae could be part of the explanation of these observations. Other factors that have been shown to display a decrease in the vascular density of the endometrium during pregnancy such as maternal age and poor nutritional status have also been associated with low birth weight (Reynolds et al., 2005). Certainly,

endometrial blood flow is important for fetal survival; women who have successful pregnancy culminating in a live birth have been shown to have significantly higher endometrial blood flow than those who suffer miscarriage (Ng et al., 2006).

The present study reveals that the vascularity of the myometrium increases with a rise in parity. These findings are at variance with what was presented by Skurupiy et al., (2010), who established that the vascularity of the pregnant uterus reduced in repeated pregnancy at the expense of more smooth muscle cell hyperplasia. The effect of litter size was not assessed in this study although it was thought to be a confounding factor. Nevertheless, in pigs, uterine blood flow has been demonstrated to have no association with the litter size (Pere and Etienne, 2000).

An ultrasonic study done in humans established that parity significantly affects uterine blood flow (Perfumo et al., 2004). According to these authors, parity notably increases the resistance index of the uterine artery as a result of retained uterine remodeling changes that had occurred in previous pregnancies. Supporting these observations is the findings of Keyes et al., (1997), who found that DNA synthesis in uterine smooth muscles cells causes their proliferation to help sustain the rise in blood flow to the uterus. In fact, progesterone has been demonstrated to be responsible for this reorganization of the uterine circulation to support pregnancy by up-regulating angiogenic markers (Milhiet et al., 1998).

In addition, the higher vascular density within the myometrium of multipara rabbits observed in this study may be part of vascular degeneration. There is evidence that parity results in alterations in vessel wall structure with resultant influence on uterine blood flow and oxygen saturation (Grüninger et al., 1998, Sabeckiene et al., 2008). The latter induces development of degenerative changes such as degenerative angiogenesis (Sabeckiene et al., 2008). In a study done on mares, Esteller-Vico et al, (2012), established that vascular degeneration in endometrial and myometrial vessels consisted of enlargement and duplication and splitting of the internal elastic lamina. According to these authors, the strongest association with vascular degeneration was parity with no association of age.

Inadequate vascular growth during early pregnancy may result in inadequate umbilical blood flow which directly affects transport of nutrients to the embryo/fetus (Grazul-Bilska et al., 2010). Additionally, ineffective vascular remodeling during pregnancy has been shown to be a prerequisite of preeclampsia (Ong et al., 2005). Pre-eclampsia is more likely to occur in the primiparae (Long et al., 1979). It is therefore plausible that the higher vascularity observed in the multipara may be protective against preeclampsia. Moreover, the higher vascularity may be part of the anatomical basis for higher likelihood of postpartum hemorrhage in multiparous females.

4.4 MYOMETRIAL SMOOTH MUSCLE ORGANIZATION AND MYOMETRIAL THICKNESS

A notable feature of the myometrium is that, as the parity rises; the myometrium is organized into more smooth muscle layers such that the multiparous myometrium displays three myometrial layer namely; the sub-endometrial zone, vascular zone and the sub-serosal zone. On the other hand, the primigravid is markedly irregular. Interlacing of myometrial fibers characterized by their irregularity contributes in controlling bleeding during the third stage of labor (Cunningham et al., 1997). It is therefore likely that this irregular arrangement is what reduces the prevalence postpartum hemorrhage in the low parity females.

It is possible that the arrangement observed in the multiparous gravid uterus contributes to the efficiency of myometrium during labour. A study done on rabbits revealed that the smooth muscle cells in the different layers possess different characteristics (Lambert et al., 1990). According to these authors, adenylate cyclase activity was higher in circular than in longitudinal smooth muscle cells. Adenylate cyclase is a second messenger in the smooth muscle contraction cascade (Kuriyama et al., 1998). Higher amounts of adenylate cyclase may imply a more forceful contraction following stimulation of the circular myometrial smooth muscle cells. Adenylate cyclase is also regulated by mechanical stimuli as it is physically attached to the cytoskeleton (Bajo et al., 2004). On the other hand, the longitudinal smooth muscle cells have a higher response to beta adrenergic isoproterenol (Lambert et al., 1990). The longitudinal smooth muscles are more efficient in relaxation given that isoproterenol is a smooth muscle relaxant. Isoproterenol causes myometrial smooth muscle relaxation via stimulation of a net efflux of calcium (Kroeger et al., 1975).

Labour is a physiologic process by which a fetus is expelled from the uterus to the outside world as a result of coordinated uterine contractions and concomitant cervical effacement and dilation (Norwitz et al., 1999). Nulliparous females are more likely to have labour dystocia and subsequent necessity for augmentation, operative vaginal delivery or caesarean section (Shields et al., 2007). Labour dystocia in nulliparous females is usually secondary to ineffective myometrial contractility (Brennan et al., 2011). On the other hand, in the multipara females, labor dystocia is likely due to obstructed labour and not inefficient uterine contraction (Cluver and Odendaal, 2010). Use of oxytocin in females of high parities is accompanied by higher rates of uterine rupture (Dawood et al., 1974, Cluver and Odendaal 2010). It has also been reported that a primigravid uterus, if a mechanical obstruction to labor exists, the uterine contractions gradually weaken and then stop. In the multiparous women, on the other hand, contractions continue until delivery or uterine rupture occurs (Neilson et al., 2003). The findings of this study as regards to the organization of the uterine musculature may contribute to explaining such observations.

This study reports increase in myometrial thickness with a rise in parity, the primigravid rabbits having a thickness of 0.44 $\pm$ 0.04 mm, while the rabbits with number of pregnancies exceeding five had a thickness of 1.004 $\pm$ mm. Closely related to the observations of the current study, are the findings of am ultrasonic study in humans that revealed that the process of labor contributed to the thickness of the lower uterine segment (Bérubé et al., 2011). According to these authors, women who had undergone previous labor had a thicker lower uterine segment than those who had a caesarean section before the onset of labor. There is evidence that myometrial thickness increases the efficiency of labour by increasing intrauterine pressure (Buhmischi et al., 2002). The thicker myometrial width in the multiparous rabbits maybe the reason why their duration of labour is much shorter. Their thicker myometrium may not be due only to thicker myocytes and blood vessels but also as a result of deposition of collagen and elastin which occurs with successive pregnancy as reported by Gunja-Smith and Woessner (1985).

4.5 CELL PROLIFERATION AND APOPTOSIS IN THE ENDOMETRIUM AND MYOMETRIUM

In the current study, the proliferative marker Ki-67 stained positively in the luminal and glandular cells of the endometrium in all the parity groups. The endothelial cells within the stroma also stained positively for this marker, the multiparous vascular channels showing the most intense staining. In the early phases of pregnancy in mares, the Ki-67 protein is present in all endometrial layers to ensure that angiogenesis and adenogenesis occur in order to support the growing conceptus (Silva et al., 2011). The more intense staining observed in the vascular channels of the multiparous rabbits may be part of the explanation why vascular density increases with parity.

The anti-apoptotic protein bcl-2 was found to stain in the luminal endometrium of all the parity groups. Jones et al., (1998) reported similar findings in humans. These authors found that progesterone treated and gravid endometria expressed high levels of bcl-2 and showed no evidence of apoptosis. On the contrary, the “receptive” non gravid endometrium in humans shows a down regulation of bcl-2 and apoptotic cell death occurs (Rango et al., 1998). According to these authors, the apoptosis observed in the endometrium in the ovulation period is expected to assist the invasion of the extravillous trophoblasts during implantation. In order to make such a conclusion accurately, more studies are required around the peri-implantation period. The current study looked at the endometrium in late pregnancy while Jones et al., (1998), studied an early pregnancy endometrium. The endometrial stromal cells and the endometrial glands hardly stained for bcl-2 with the exception of the multiparous endometrium, which also portrayed intense staining in the endothelial cells of vascular channels within the endometrial stroma.

In the present study, staining for the Ki-67 protein within the myometrium was such that the sections in the mid-cornual parts and the fallopian tube stained positively in the primiparous and multiparous myometria compared to the intermediate parity group. The parts of the myometrium that stained positively were stromal cells and vascular elements. The cervical fibromuscular area hardly stained for this marker. Lei et al., (2012), reported that the hormone progesterone as well as DNA damage both encourages uterine cell proliferation. Multiparity has been shown to result in endothelial dysfunction via increasing oxidative stress in this tissue (Tawfiq et al., 2008). For this reason, the intense proliferation in the multiparous uterus shown in this study may be as a result of DNA damage. On the other hand, maternal hormone profile has been reported to be affected by parity (Arslan et al., 2006), with higher levels of hormones such as estradiol, progesterone, HCG, AFP and prolactin being noted in primigravid females. The higher progesterone may explain the findings of this study in the primiparous myometrial proliferation.

4.6 LIMITATIONS OF THE STUDY

One of the probable confounders of this study was the aspect of litter size. It is possible that litter size affects the structure of the uterus. Nonetheless, this confounder was present in all the groups in this study. Other studies can look into effect of litter size on the uterus. The fact that there may be inter-individual differences regarding anatomical structures may warrant further exploration of this concept with more studies looking into parity.

CONCLUSION

The primigravid uterus is characterized by higher density of endometrial glands, reduced vascular density of the endometrium and myometrium and reduced myometrial thickness. Myometrial smooth muscle layers become more organized as parity increases. This architecture of smooth muscles as parity rises, may be the reason why the multiparous uterus is efficient for fetal expulsion. The higher vascularity in the higher parity group was as a result of both increased proliferation and reduced apoptosis evidenced by intense staining of the proliferation marker Ki-67 and the anti-apoptotic protein Bcl-2 in this group. The increased vascularity observed in the multiparous rabbits provides an explanation of higher likelihood of postpartum hemorrhage in the higher parity females.

SUGGESTIONS FOR FUTURE STUDIES

As an expansion of the findings of this study, future studies can look into the following;

1. Effect if liter number on uterine structure
2. Effect of parity on total endometrial size/volume
3. The type of angiogenesis that occurs in uterine layers during pregnancy

REFERENCES

1. Ababneh MM, Degafa T. Ultrasonic assessment of puerperal uterine involution in Balady goats. *J Vet Med A Physiol Pathol Clin Med.* 2005; 52: 244-248.
2. Adams JM, Cory S. The bcl-2 protein family; arbiters of cell survival. *Science.* 1998: 28; 281: 1322-1326.
3. Akinloye AK. Oke BO. Characterization of the Uterus and Mammary Glands in the Female African Giant Rats (Cricetomys gambianus, Waterhouse) in Nigeria. *Int J Morphol*. 2010; 28: 93-96.
4. Albrektsen G, Hendi I, Wik E, Salvesen HB. Parity and time interval since childbirth influence survival in endometrial cancer patients. *Int J Gynecol Cancer.* 2009; 19: 665-669.
5. Allen WR, Gower S, Wilsher S. Immunohistochemical localization of vascular endomethelial growth factor VEGF and its two receptors (flt I and KDR) in the endometrium and placenta of mare during the oestrous cycle and pregnancy. *Reprod Domest Anim.* 2007; 42:516-526.
6. Amira ABK, Zuki ABZ, Goh YM, Noordin MM. Histological changes in the endometrial Sprague-Dawley rats under supplementation levels of n-6:n-3 fatty acid ratio. *Afr J Biotechnol.* 2011: 10: 5524-5528.
7. Ananth CV, Wilcox AJ, Savitz DA, Bowes WA Jr, Luther ER. Effect of maternal age and parity on the risk of uteroplacental bleeding disorders in pregnancy. *Obstet Gynecol.* 1996; 88: 511-516.
8. Argente MJ, Santacreu MA, Climent A, Blasco A. Influence of available uterine space per fetus on fetal development and prenatal survival in rabbits selected for uterine capacity. 2006. *Livest Sci.* 2006; 102: 83-91.
9. Arias-Stella J. Atypical endometrial changes associated with presence of placental tissue. *Arch Pathol.* 1954; 58; 112-128.
10. Arslan AA, Zeleniuch-Jacqotte A, Lukanova A, Afanasyeva Y, Katz J, Levitz M, Del Priore G, Toniolo P. Effects of parity on pregnancy hormonal profiles across ethnic groups with diverse incidence on breast cancer. *Cancer Epidemiol Biomarkers Prev.* 2006; 15: 2123-2130
11. Arulkumaran S, Gibb DM, Lun KC, Heng SH, Ratnam SS. The effect of parity on uterine activity in labour. *Br J Obstet Gynaecol.* 1984; 91: 843-848.
12. Baird DD, Dunson BD. Why is parity protective for uterine fibroids? *Epidemiology.* 2003; 14: 247-250.
13. Bai J, Wong FW, Bauman A, Mohsin M. Parity and Pregnancy outcomes. *Am J Obstet Gynecol.* 2002; 186: 274-278.
14. Bartelmez GW. Histologic studies on the menstruating mucous membrane. *Contrib Embryol.* 1993; 142: 142-157.
15. Bajo AM, Prieto JC, Valenzuela P, Maritinez P, Menor C, Marina A, Vazquez J, Gijarro LG. Association of adenylate cyclase with actin-like protein in the human myometrium. *Gynecol Endocrinol.* 2004; 18(2): 89-96.

16. Baecker V. Image processing and analysis with Image J and MRI Cell Image Analyzer. *Montpellier RIO Imaging*. 2010; 1-93
17. Baumans V. Use of animals in experimental research; an ethical dilemma. *Gene ther.* 2004; 11: 64-66.
18. Begum S. Age and parity related problems outcome of labour in grand multiparas. *Pakistan J Med Res.* 2003; 42: 179-184.
19. Benacerraf BR, Shipp TD, Lyons JG, Bromley B. Width of the normal uterine cavity in premenopausal women and effect of parity. *Obstet Gynecol.* 2010; 116: 305-310.
20. Berube L, Arial M, Gagnon G, Brassard N, Boutin A, Bujold E. Factors associated with lower uterine segment thickness near term in women with previous caesarean section. *J Obstet Gynaecol Can.* 2011; 33: 581-587.
21. Blix E, Pettersen Sh, Ericksen H, Royset B, Pedersen EH, Oian P. Use of oxytocin augmentation after spontaneous onset of labour. *Tidsskr Nor Laege Foren* . 2002; 122: 1359-1362.
22. Bracher V, Mathias S, Allen WR. Influence of chronic degenerative endometritis (endometrosis) on placental development in the mare. *Equine Vet J* 1996; 28: 180-188.
23. Brennan DJ, McGee SF, Rexhepaj E, O'Connor DP, Robson M, O'Herlihy C. Identification of myometrial molecular profile for dystotic labor. *BMC Pregnancy Childbirth.* 2011; 11:74: 1471-2393-11-74.
24. Brown HK, Stoll BS, Nicosia SV, Fiorica JV, Hambley PS, Clarke LP, Silbiger ML. uterine junctional zone; correlation between histologic findings and MR imaging. *Radiology.* 1991; 179: 409-413.
25. Buhmischi CS, Buhimschi IA, Malinow AM, Kopelman JN, Weiner CP. The effect of fundal pressure manouvre on the intrauterine pressure in second stage labour. *BJOG.* 2002; 109: 520-526.
26. Buhmischi CS, Buhmschi IA, Malinow AM, Weiner CP. Myometrial thickness during labour and immediate postpartum. *Am J Obstet Gynecol.* 2003; 188: 553-559.
27. Buhmischi CS, Buhimschi IA, Wehrum MJ, Molaskey-Jones S, Stafianaki AK, Pettker CM, Thung S, Campbell KH, Dulay AT, Funai EF, Bahtiyar MO. Ultrasonographic evaluation of myometrial thickness and prediction of successful external cephalic version. *Obstet Gynaecol.* 2011; 118:913-920.
28. Bujold E, Gauthier RJ. Neonatal morbidity associated with uterine rupture. What are the risk factors? *Am J Obstet Gynecol.* 2002; 186: 311-314.
29. Cavaillé F, Cabrol D, Ferre F. Human myomstrial smooth muscle cells and cervical fibroblasts in culture; a comparative study. *Methods Mol Med.* 1996; 2:335-344.
30. Celeste P, Durnwald MD, Brian MM. Myometrial thickness according to uterine site, gestational age and prior caesarean delivery. *J Matern Fetal Neonatal Med.* 2008; 21: 247-250.

31. Cluver CA, Odendaal HJ. Oxytocin augmentation: poison or potion to the multipara? *Obstetrics and Gynaecology Forum*. 2010; 20: ISSN1027-9148.
32. Cooke PS, Spencer TE, Bartol FF, Hayanashi K. Uterine glands development function and experimental model systems. *Mol Hum Reprod.* 2013: (Epub ahead of print). PMID: 23619340.
33. Cruz YP, Selwood L, Histological differences between gravid and non-gravid uteri in the dasyurid marsupial, sminthopsis macroura (spencer). *J Reprod Fertil.* 1997; 11: 319-325.
34. Cunningham FG, MacDonald PC, Gant NF, et al: Maternal adaptation to pregnancy. In: *Williams Obstetrics*. 20th Ed. Stamford, CT, Appleton & Lange. 1997, p 191.
35. Davies J, Hoffman LH. Studies on the progestational endometrium of the rabbit I. Light microscopy, day 0 to day 13 of gonadotropin-induced pseudopregnancy. *Am J Anat.* 1973. 137:423-445.
36. Dawood MY, Ng R, Ratnam SS. Oxytocin stimulation and uterine rupture in the grandmultipara. *S M J.* 1994; 15: 40-44.
37. Degafa T, Ababneh MM, Moustafa MF. Uterine involution in the post-partum Balady goat. *Vet Archiv*. 2006; 76:119-133.
38. Degani S, leibovitz Z, Shapiro I, Gonen R, Ohel G. Myometrial thickness in pregnancy: longitudinal sonographic study. *J Ultrasound Med.* 1998; 17: 661-665.
39. Deligdisch L. Effects of hormone therapy on the endometrium. *Mod Pathol.* 1993; 1: 94-106.
40. Dolgikh OV, Agavonov IUV, Zashikhin AL. Adaptive transformation of rat myometrium with progression of pregnancy after parturition. *Morphologia.* 2012; 142:59-63
41. Drury RAB, Wallington EA, Cameron R. In: *Carleton's Histological Techniques*.4th edition. Newyork. Oxford University Press 1967; 166-181.
42. Eng J. Sample size estimation: A glimpse beyond simple formulas. *Radiology.* 2003; 230: 602-612.
43. Esteller-Vico A, Liu IK, Couto S. Uterine Vascular degeneration is present throughout the uterine wall of multiparous mares. Colinearity between elastosis, endometrial grade, age and parity. *Theriogenology*. 2012; 78: 1078-1084.
44. Farrer-Brown G, Beilby JOW, Tarbit MH. The blood supply of the uterus; arterial vasculature. *J. Obstet Gynaecol Br commonw.* 1970; 77: 682-689.
45. Favaro RR, Salgado RM, Raspantini PR, Fortes ZB, Zorn TMT. Effects of long-term diabetes on the structure and cell proliferation of the myometrium in the early pregnancy of mice. *Int. J Exp Pathol.* 2010: 91(5):426-435.
46. Ferenczy A, Mutter GL. The endometrial cycle. *Glob. Libr. Women's med.* 2008; DOI 10. 3843/GLOWN. 10293(ISSN: 1756-2228).
47. Finn CA, Martin L. Hormonal Control of the secretion of endometrial glands. *J Endocrinol.* 1976; 71:273-274.

48. Fuch A, Fuch F, Husslein P et al., Oxytocin receptors and human parturition a dual role for oxytocin for in the initiation of labor. *Science*. 1982; 215: 1396-1398.
49. Fuch AR, Fuch f, Husslein P, Soloft MS. Oxytocin receptors in the human uterus during pregnancy and parturition. *Am J obstet Gynecol.* 1984; 150: 734-741.
50. Gerstenberg C, Allen WR, Stewart F. Cell proliferation patterns in the equine endometrium throughout the non-pregnant cycle. *J Reprod Fertil.* 1999; 116: 167-175
51. Girling JE, Lederman FL, Waller LM, Rogers PA. Progesterone, but not oestrogen, stimulates vessel maturation in the mouse endometrium. *Endocrinology*. 2007; 148: 5433-5441.
52. Golan A, Sanbank O, Rubin A. rupture of the pregnant uterus. *Obstet Gynaecol* 1980; 56: 549-554.
53. Goodger AM, Rogers PA. Uterine endothelial cell proliferation before and after embryo implantation in rats. *J Reprod Fertil.* 1993; 99: 451-457.
54. Graham JD, Clarke CL. Physiological action of progesterone in target tissues. *Endocr Rev.* 1997; 18: 502-519.
55. Gray CA, Taylor KM, Ramsey WS, Hill JR, Bazer FW, Bartol FF, Spencer TF. Endometrial glands are required for pre-implantation conceptus elongation and survival. *Biol Reprod.* 2001a; 64:1608-1613.
56. Gray CA, Bartol FF, Taeleton BJ, Wiley AA, Johnson GA, Bazer FW. Developmental biology of uterine glands. *Biol Reprod.* 2001b; 65:1311-1323.
57. Gray CA, Burghardt RC, Johnson GA, Bazer FW, Spencer TE. Evidence that absence of endometrial gland secretions in uterine gland knockout ewes compromises conceptus survival and elongation. *Reproduction*. 2002; 24: 289-300.
58. Gray CA, Stewart MD, Johnson GA, Spencer TE. Postpartum uterine involution in sheep: histoarchitecture and changes in endometrial gene expression. *Reproduction.* 2003; 125:185-198.
59. Grazul-Bilska AT, Borowicz PP, Johnson ML, Minten MA, Bilski JJ, Wroblewski R, Redmer DA, Reynolds LP. Placental development during early pregnancy in sheep: Vascular growth and expression of angiogenic factors in maternal placenta. *Reproduction.* 2010; 140: 165-174.
60. Grompel A, Sabourin JC, Martin A, Yaneva H, Audouin J, Decroix Y, Poitout P. Bcl-2 expression in normal endometrium during the menstrual cycle. *A J P.* 1994; 144: 1195-1202.
61. Groothius PG, Dassen HHNM, Romano A, Punyadeera C. Estrogen and the endometrium: Lesson learned from gene expression profiling in rodents and humans. *Hum Reprod Update.* 2007; 13: 405-417.
62. Grüninger B, Schoon HA, Schoon D, Menger S, Klug E. Incidence and morphology of endometrial angipathies in mares in relationship to age and parity. *J Comp Pathol.* 1998; 119: 293-309.

63. Gunja-Smith Z, Woessner JF. Content of the collagen and elastin cross-links pyridnoline and the desmosines in the human uterus in various reproductive states. *Am J Obstet Gynecol.* 1985; 153: 92-95.
64. Hafez ES, Tsutsumi Y. Changes in endometrial vascularity during implantation and pregnancy in the rabbit. *Am J Anat.* 1966; 118:249-82.
65. Hafez ES. In: *Reproduction and Breeding techniques for Laboratory Animals.* Phildelphia. USA, Lea & Febiger. 1970. 67.
66. Hertelendy F, Zakar T. Regulation of myometrial smooth muscle functions. *Curr Pharm Des*. 2004; 10: 2499-517.
67. Hempstock J, Cindrova-Davies T, Jauniax E, Burton GJ. Endometrial glands as a source of nutrients, growth factors and cytokines during the first trimester of human pregnancy: A morphological and immunochemical study. *Reprod Biol Endocrin.* 2004; 2:58 doi :0.1 186/1477-7827-2-58.
68. Hinkula M, Pukkala E, Kyyrinen O, Kauppila A. Grand multiparity and incidence of the endometrial cancer: a pupulation-based study in Finland. *Int J Cancer.* 2002; 98: 912-915.
69. Huang CC, Orvis GD, Wang Y, Behringer RR. Stromal to epithelial transition during postpartum endometrial regeneration. 2012; PLoS One. Epub ahead of print. doi: 10. 1371.
70. Intan-shameha AR, Zuki ABZ, Nornajibah K, Zamri-Saad M. Microscopic evaluation of uterine mucosa in pregnant and non-pregnant rats. *J Anim Vet Adv.* 2005; 4: 590-594
71. Jacobson L, Rienner RK, Goldfield AC, Lykins D, Siiter PK, Roberts JM. Rabbit myometrial oxytocin receptors and alpa 2-adrenergic receptors are increased by estrogen but are differentially regulated by progesterone. *Endocrinology.* 1987; 120: 1184-1189.
72. Jain V, Saade GR, Garfield RE. Structure and function of the Myometrium. *Adv Organ Biol.* 2000; 8: 215-246.
73. Jeyasuria P, Wetzel J, Bradley M, Subedi K, Condon JC. Progesterone-regulated caspase 3 action in the mouse may play a role in uterine quiescent during pregnancy through fragmentation of uterine myocyte contractile proteins. *Biol Reprod.* 2009: 80; 929-944.
74. Jeyasuria P, Subedi K, Condon JC. Elevated levels of uterine anti-apoptotic signaling may activate NKFB and potentially confer resistance to caspace 3-mediated apoptotoc cell death during pregnancy in mice. *Biol Reprod*. 2011; 85: 417-424.
75. Jones RK, Searle RF, Stewart JA, Turner S, Bulmer JN. Apoptosis, bcl-2 expression, and proliferative activity in human endometrial stroma, and endometrial granulated lymphocytes. *Biol Reprod.* 1998; 58: 995-1002.
76. Jones TR. In. *General Outline of the Organization of the Animal Kingdom and Manual of Comparative Anatomy.* London. J. Van Voorst, 1861. 3rd Edition. 2013. 537.
77. Kandiel MMM, Watanabe G, Sosa GA, El-Ross MEAA, Abdel-Ghaftar AE, Li JY, Manabe N, Azab AESI, Taya K. Profiles of circulating steroid hormones, Gonadotropins, immunoreactive

inhibin and prolactin during pregnancy in goats and immunolocalization of inhibin subunits, steroidogenic enzymes and prolactin in the corpus luteum and placenta. *J Reprod Develop*. 2010; 56: 243-250.

78. Kaeoket K, Persson E, Dalin AM. The sow endometrium at different stages of the oestrous cycle: studies on morphological changes and infiltration by cells of the immune system. *Anim Reprod Sci.* 2002; 73:89-107.
79. Keyes LE, Majack R, Dempsey EC, Moore LG. Pregnancy stimulation of DNA synsthesis and uterine blood flow in the guinea pig. *Pediatr Res. 1997;* 41: 708-715.
80. Keys JL, King GJ. Morphological evidence for increased uterine vascular permeability at the time of embryonic attachment in the pig. *Biol Reprod.* 1988; 39: 473-487.
81. Kiracofe GH. Uterine involution: its role in regulating postpartum intervals. *J Anim Sci* . 1980; 51:16-28
82. Krajničáková M, Bekeová E, Lenhardt L', Ciganková V, Valocky I, Maraček I. Microscopic analysis of the endometrium in postparturient ewes. *Acta Vet BRNO.* 1999; 68:9-12.
83. Kroeger EA, Marshall JM, Bianchi CP. Effect of isoproterenol and D-600 on calcium movements in rat myometrium. *JPET.* 1975; 193: 309-316.
84. Kuriyama H, Kitamura K, Itoh T, Inoue R. Physiologic features of visceral smooth muscle cells with reference to receptors and ion channels. *Physiol Rev.* 1998; 78: 812-889.
85. Lambert FL, Pelletier G, Dufous M, Fortier MA. Specific properties of smooth muscle cells from different layers of rabbit myometrium. *Am J Physiol Cell Physiol*. 1990: 258; C794-C802.
86. Langlois PL. The size of the normal uterus. *J. Reprod Med.* 1970; 4: 220.
87. Lefranc AC, Allen WR. Influence of breed and oestrous cycle on endometrial gland surface density in the mare. *Equine Vet J.* 2007: 39:506-510.
88. Lei W, Feng Xh, Deng WB, Ni H, Zhang ZR, Jia B, Yang XL, Wang TS, Liu JL, Su RW, Liang XH, Qi QR, Yang ZM. Progesterone and DNA damage encourage uterine cell proliferation anad decidualization through upregulating ribonucleotide reductase 2 expression during early pregnancy in mice. *J. Biol. Chem.* 2012: 287; 1574-92.
89. Lessey BA. The role of the endometrium during embryo implantation. *Human Reprod*. 2000; 15:39-50
90. Leung St, Warthes DC. Oestradiol reguklation of oxytocin receptor expression in cyclic bovine endometrium. *J. Reprod. Fertil.* 2000; 119: 287-292.
91. Liu L, Li Y, Xie N, Shynlova O, Challis JR, Slater D, Lye S, Dong X. Proliferative action of the androgen receptor in human uterine myometrial cells--a key regulator for myometrium phenotype programming. *J Clin Endocrinol Metab.* 2013; 98: 218-227.
92. Lobel BL, Deane HW. Enzymatic Activity Associated with postpartum involution of the uterus and with its regression after hormone withdrawal in the rat. *Endocrinology.* 1962; 70: 567-578.

93. Long PA, Abell DA, Beischer NA. Parity and Pre-eclampsia. *Aust NZJ Obstet Gynecol.* 1979; 19:2003-2006.
94. Lye SJ, Ou CW, Feoh TG, Erb G, Stevens Y, Capser R, Patel FA, Challis JRG. The molecular basis of labour and tocolysis. *Fetal Matern Med Rev.* 1998; 10: 121-136.
95. Majoko F, Nyström L, Munjanja SP,Mason E, Lindmark G. Relation of Parity to Pregnancy Outcome in a Rural Community in Zimbabwe. *Afr J Reprod Health.* 2004; 8: 198-206.
96. Makanya AN, Hlushchuk R, Djonov VG. Intussusceptive angiogenesis and its role in vascular morphogenesis, patterning and remodeling. *Angiogenesis.* 2009; 12: 113-123
97. Maksem JA, Meiers I, Robboy SJ. A primer of endometrial cytology with histological correlation. *Diagn Cytopathol.* 2007; 35: 817-844.
98. Malavankar DV, Gray RH, Trivedi CR. Risk factors for preterm and low birthweight in Ahmedabad India. *Int J Epidemiol.* 1992; 21: 263-272.
99. Marth C, Windbitcher G, Petru E, Dirschlmayer W, Obermair A, Czerwenka K, Muller-Holzer, Dapunt O. Parity as an independent prognostic factor in malignant mixed mesordermal tumours of the endometrium. *Gynecol Ortcol.* 1997; 64: 121-125.
100. Maruyama T, Masuda H, Ono M, Kajitani T, Yoshimuru Y. Human uterine stem/progenitor cells: their possible role in uterine physiology and pathology. *Reproduction.* 2010; 140: 11-22.
101. Meier-Abt F, Milani E, Roloff T, Brinkaus H, Duss S, Meyer DS, Klebba I, Balwierz PJ, van Nimwegen E, Bentirez-Alj M. Parity induces differentiation and reduces wnt/Notch signaling ratio and proliferation potential of basal stem/progenitor cells isolated from mouse mammary epithelium. *Breast Cancer Res.* 2013; 15: R36 (Epub ahead of print).
102. Milhiet PE, Vacherot F, Camelle JP, Barritault D, Camelle D. Upregulation of the angiogenic factor heparin affin regulatory peptide by progesterone in the rat uterus. *J Endocrinol.* 1998; 158: 389-399.
103. Moll W, Espach A, Wrobel KH. Growth of mesometrial arteries in guinea pigs during pregnancy. *Placenta.* 1983; 4:11-123.
104. Moreira PM, Mendes V, Dia A, Diouf A, Diadhiou F, Moreau JC. The histological aspect of the uterine vein wall according to age and parity. *Dakar Med*. 2008; 53:154-161.
105. Moyer DL, Felix JC. The effect of progesterone and progestins on endometrial proliferation. *Int J Gynecol pathol.* 1998; 57: 399-403.
106. Nasar A, Rahman A. Hormonal changes in the uterus during pregnancy-lessons from the Ewe: A Review. *J Agric Rural Dev.* 2006; 4: 1-7.
107. Negishi H, Kishinda T, Yamada H, Hirayama E, Mikuni M, Fujimoto S. Changes in uterine size after vaginal delivery and caesarean section determined by vaginal sonography in pueperium. *Arch.Gynecol Obstet.* 1999; 263: 13-16.
108. Neilson JP, Lavender T, Quenby S, Wray S. Obstructed labour. *Brit Med Bull.* 2003; 67: 191-204.

109. Ng EHY, Chan CCW, Tang OS, Yeung WSB, Ho PC. Factors affecting endometrial and subendometrial blood flow measured by three-dimensional power Doppler ultrasound during IVF treatment. *Hum Reprod.* 2006; 21:1062-1069.

110. Ng EHY, Chan CCW, Tang OS, Yeung WSB, Ho PC. Endometrial and subendometrial vascularity is higher in pregnant patients with live birth following ART than in those who suffer a miscarriage. *Hum Reprod.* 2007; 22: 1134-1141.

111. Nicolae A, Preda O, Nogales FF. Endometrial metaplasias and reactive changes: a spectrum of altered differentiation. *J Clin Pathol.* 2010. 10; 1136/jcp

112. Norwitz ER, Robinson J, Challis JRG. The control of labor. *N Eng J Med.* 1999; 341: 660-666.

113. Ocak S, Ogun S, Onder H. Relationship between placental traits and maternal intrinsic factors in sheep. *Anim Reprod* Sci. 2013; 139:31-37.

114. Ogle TF, Dai D, George P. Progesterone-regulated determinants of stromal cell survival and death in uterine deciduas are linked to protein C kinase activity. *Steroids.* 1999; 64: 628-623.

115. Olayemi O, Omigbodun AA, Obajimi MO, Odukogbe AA, Agunloye AM, Aimakhu CO, Okonlola MA. Ultrasound assessement of the effect of parity on postpartum uterine involution. *J. Obstet Gynecol.* 2002; 4: 381-384.

116. Ong SS, Baker PN, Mayhew TM, Dunn WR. Remodelling of myometrial radial arteries in preeclampsia. *Am J Obstet Gynecol.* 2005; 192: 572-579.

117. Ono M, Maruyama T, Yoshimura Y. Regeneration and adult stem cells in the human reproductive tract. *Stem Cells & Cloning.* 2008: 23-29.

118. O'shea JD, Wright PJ. Involution and regeneration of the endometrium following parturition in the ewe. *Cell Tissue Res.* 1984; 236; 477-485.

119. Osol G, Mandala M. Maternal uterine vascular remodeling during pregnancy. *Physiology.* 2009; 24:58-71.

120. Otsuki Y. Apoptosis in human endometrium: apoptotic detection methods and signaling. *Med Electron Microsc.* 2001: 34: 166-173.

121. Pace D, Morrison L, Bulmer JN. Proliferative activity in the endometrial stromal granulocytes throughout menstrual cycle and early pregnancy. *J Clin Pathol* 1989; 42:35-39.

122. Palmer SK, Zamudio S, Coftin C, Parker S, Stamm E, Moore LG. Quantitative estimation of human uterine blood flow and pelvic blood flow redistribution in pregnancy. *Obstet Gynaecol.* 1992; 80:1000-1006

123. Parry HJ. The vascular structure of the extraplacental uterine mucosa of the rabbit. *J Endocrinol*. 1950: 7:86-99

124. Père MC, Etienne M. Uterine blood flow in sows: effects of pregnancy stage and litter size. *Reprod Nutr Dev.* 2000; 40: 369-382.

125. Prefumo F, Blide A, Sairam S, Penna L, Hollis B, Thilaganathan B. Effect of parity on second trimester artery Doppler flow velocity and waveforms. *Ultrasound Obstet Gynecol.* 2004; 23 (1): 46-49.

126. Qureshi B, Inafuku K, Oshima K, Masomoto H, Kanazawa K. Ultrasonographic evaluation of the lower uterine segment to predict the integrity and quality of caesarean scar during pregnancy: A prospective study. *Tohuku J Exp Med.* 1997; 183: 55-65.

127. Ramsey ME. Anatomy of the human uterus. In: Chard T, Grudzinskass G, editors. *The uterus.* Cambridge University Press. London. 1994; 18-29.

128. Rango U, Classen-Linke I, Krusche CA, Beier HM. The receptive endometrium is characterized by apoptosis in the glands. *Hum Reprod.* 1998; 113; 3177-3189.

129. Rehman KS, Yin SU, Mayhew A, Word RA, Rainey WE. Human myometrial adaptation to pregnancy:cDNA microarray gene expression profiling of myometrium from non-pregnant and pregnant women. *Mol Hum Reprod.* 2003: 9:681-700.

130. Reynolds LP, Redmer DA. Growth and microvascular development of the uterus during early pregnancy in ewes. *Biol. Reprod.* 1992; 42: 698-708.

131. Reynolds LP, Redmer DA. Angiogenesis in the placenta. *Biol. Reprod.* 2001; 64:1033-1040.

132. Reynolds LP, Borowicz PP, Vonnahme KA, Johnson ML, Grazul-Bilska AT, Redmer DA, Caton JS. Placental angiogenesis in sheep models of compromised pregnancy. *J Physiol.* 2005; 565: 43-58.

133. Roberts RM, Bazer FW, Thatcher WW. Biochemical interactions between blastocyst and endometrium in large domestic animals. *J Biosci.* 1984: 6 (2): 63-74.

134. Rogers PAW. Structure and function of endometrial blood vessels. *Hum Reprod Update.* 1996; 2:57-62.

135. Rosario GX, D'Souza SJ, Manjramkas DD, Parmar V, Puri CP, Sachdeva G. Endometrial modifications during early pregnancy in bonnet monkeys (macaca radiata). *Reprod Fert Develop.* 2007; 20:281-294

136. Sabeckiene J, Aniuliene A, Gruys E. Uterine blood vessels angipathies in mares. *Veterinarija Ir Zootechnika T*. 2008; 42; 1392-2130.

137. Scherle W. A simple method for volumetry of organs in quantitative stereology. *Mikroskopie.* 1970; 26: 57-60.

138. Scholzen T, Gerdes J. The Ki-67 protein: from the known to the unknown. *J cell Physiol*. 2000: 182: 311-322

139. Shao J, Li MQ, Meng YH, Chang KK, Wang Y, Zhang L, Li DJ. Estrogen promotes the growth of decidual stromal cells in human early pregnancy. *Mol Hum Reprod.* 2013 (Epub ahead of print). PMID: 23649593.

140. Shechter Y, Levy A, Wiznitzer A, Zlotnik A, Sheiner E. Obstetric complications in grand and great grand multiparous women. *J Matern fetal Neonatal Med.* 2010; 23: 1211-1217.

141. Shields SG, Ratcliffe SD, Fontaine P, Leeman L. Dystocia in nulliparous Women. *Am Fam Physician*. 2007; 1617-1678.

142. Shynlova O, Oldenhof A, Dorogin A, Xu Q, Mu J, Nashman N & Lye SJ. Myometrial apoptosis: activation of the caspase cascade in the pregnant rat myometrium at midgestation. *Biol Reprod*. 2006; 74: 839–849.

143. Shynlova O, Nedd-Roderique T, Li Y, Dorogin A, Lye SJ. Myometrial immune cells contribute to term parturition preterm labour and post-partum involution in mice. *J Cell Mol Med.* 2013; 17: 90-102

144. Silva LA, Klein C, Ealy AD, Sharp DC. Conceptus-mediated endometrial vascular changes during pregnancy in mares: an anatomic, histomorphometric, and vascular endothelial growth factor receptor system immunolocalization and gene expression study. *Reproduction.* 2011; 42: 593-603.

145. Skurupiy VA, Obedinskaya KS, Nadeev AP. Structural manifestation of mechanisms of myometrium involution after repeated pregnancies in mice. *Bull Exp Biol Med;* 2010; 149: 554-558.

146. Solomons B. The dangerous multipara. *The Lancet*. 1934; 2: 8-11.

147. Spencer TE, Gray A. Sheep Uterine gland knockout (UGKO) model. *Methods Mol Med.* 2006; 121:85-94.

148. Stewart EA. Uterine fibroids. *The Lancet.* 2001; 357: 293-298.

149. Stubbs TM, Oxytocin for labor induction. *Clin Obstet Gynaecol.* 2000; 43: 489-494.

150. Sullivan FM, Tucker JF. Uterine blood flow in the pregnant rabbit. *J Reprod Fertil.* 1975; 42: 239-250.

151. Suzuki A, Kariya M, Matsumara N, Baba T, Yagi H, Mandai M, Konishi I, Fujii S. Expression of P53 and P21 (WAF-1), apoptosis, and proliferation of smooth muscle cells in normal myometrium during the menstrual cycle; implication of DNA damage and repair for leiyomyoma development. *Med Mol Morphol.* 2012; 45: 214-221.

152. Tabb TN, Garfield RE, Thilander G. Physiology of myometrial function; Intercellular coupling and its role in uterine contractility. *Fetal Matern Med Rev*. 1991; 3: 169-183.

153. Tawfiq H, Cena J, Schultz R, Kaufman S. Role of oxidative stress in multiparity induced endothelial dysfunction. *Am J Physiol Heart Circ Physiol.* 2008. 295: H1736-1742.

154. Tsujimoto Y. Role of anti-apoptotic proteins BCL-2 protein in spinal muscular atrophy. *J. Neural Transm.* Suppl. 2000; 58: 41-42.

155. Tsujimoto Y. Role of Bcl-2 family proteins in apoptosis, apoptosomes or mitochondria? *Genes Cells.* 1998; 3: 697-707.

156. Vang R, Barnes R, Wheeler DT, Strauss BL. Immunohistochemical staining for Ki-67 and P53 helps distinguish endometrial Arias-Stella reaction from high-grade carcinoma including clear cell carcinoma. *Int J Gynecol Pathol.* 2004; 23: 223-233.

157. Wang CK, Robinson RS, Flint AP, Mann GE. Quantitative analysis of changes in endometrial gland morphology during the bovine oestrous cycle and their association with progesterone levels. *Reproduction.* 2007; 134: 365-371.

158. Weeks AD, Wilkinson N, Arora DS, Duffy SR, Wells M, Walker JJ. Menopausal changes in the Myometrium. An investigation using a GnRH agonist. *Int J Gynecol Pathol*. 1999; 18: 226-232.

159. Weston G, Rogers PAW. Endometrial angiogenesis. *Baillière's clin obstet gynecol.* 2000. 14: 919-936.

160. Wheeler DT, Bristow RE, Kurman RJ. Histologic alterations in endometrial hyperplasia and well differentiated carcinoma treated with progestins. *AM J Surg Pathol.* 2007; 31: 988-998

161. Williams PL, Banister LH, Berry MM, Collins P, Dyson M, Dussek JE, Fergusson MWJ (editors). In: *Gray's Anatomy.* London. Churchill Livingstone. 38th edition. 1995; 1869-1874.

162. Wilsher S, Allen WR. The effects of maternal age and parity on placental and fetal development in the mare. *Equine Vet J.* 2003; 35: 476-483.

163. Yasmeen L, Rasheed T, Syed S. Is grand multiparity still a risk factor for obstetric complications? *Ann Pak Inst Med*. Sci. 2010; 6: 58-61.

164. Young SL. Progesterone function in human endometrium: clinical perspectives. *Semin Reprod Med*. 2010. 28: 015-016.

165. Zduńczyk S, Milewski S, Barański W, Janowski T, Szczepański W, Jurczak A, Raś A, Leśnik M. Postpartum uterine involution in primiparous and pluriparous polish longwool sheep monitored by ultrasonography. *Bull Vet Inst Pulawy.* 2004; 48: 255-257.

166. Zhang J, Deng LX, Zhang HL, Hua GH, Han L, Zhu Y, Meng XJ, Yang LG. Effects of parity on uterine involution and resumption of ovarian activities in postpartum Chinese Holstein cows. *J Dairy Sci.* 2010; 93: 1979-1986.

APPENDIX:

DATA SHEET

1. Study number……
2. Parity
   - Primigravid rabbits (Group 1)
   - Para 1-Para 3
   - Para ≥ 4
3. Calculated Endometrial gland density
   a. 1st measurement……..
   b. 2nd measurement……
   c. 3rd measurement……
   d. 4th measurement……
   e. 5th measurement……
4. Endometrial gland circumference
   a. 1st measurement……..
   b. 2nd measurement……
   c. 3rd measurement……
   d. 4th measurement……
   e. 5th measurement……
5. Calculated endometrial vascular density
   a. 1st measurement……..
   b. 2nd measurement……
   c. 3rd measurement……
   d. 4th measurement……
   e. 5th measurement……
6. Calculated myometrial vascular density
   a. 1st measurement……..
   b. 2nd measurement……
   c. 3rd measurement……
   d. 4th measurement……
   e. 5th measurement……
7. Myometrial thickness
   a. 1st measurement……..
   b. 2nd measurement……
   c. 3rd measurement……
   d. 4th measurement……

e. 5th measurement……

8. Distribution of the proliferation ki-67 marker in the endometrium
   ……
   ……
   ……
9. Distribution of the proliferation ki-67 marker in the myometrium
   ……
   ……
   ……
10. Distribution of the anti-apoptotic protein bcl-2 marker in the endometrium
    ……
    ……
    ……

11. Distribution of the anti-apoptotic protein bcl-2 marker in the myometrium
    ……
    ……
    ……